FLUIDYNE ENGINEERING CORPORATION

DETERMINATION OF DISCHARGE AND THRUST COEFFICIENTS OF A CHOKED ASME NOZZLE FROM EXIT FLOW SURVEYS (ADDITIONAL TESTS)

by

James S. Holdhusen
Donald Perusse

Conducted for

General Electric Company
Cincinnati, Ohio

G. E. Purchase Order No. 200G230285
FluiDyne Project 0470

September 1965

Approved by: James L. Grunnet
James L. Grunnet
Project Engineer

Nicholas C. Helm
Program Planner

Owen P. Lamb
Program Manager

TABLE OF CONTENTS

DEFINITION OF SYMBOLS

A	Local Area	square feet
A_e	Nozzle Exit Area	square feet
a	Local Speed of Sound	feet/second
C_D	Discharge Coefficient	
C_s	Stream Thrust Coefficient	
C_V	Thrust Coefficient Calculated Using p_s at Nozzle Exit	
F	Nozzle Exit Stream Thrust	pounds
G	Exhaust Thrust $(F - p_a A_e)$	pounds
M	Mach Number	
$\dot{m}$	Mass Flow	slugs/second
p_a	Static Pressure in Plenum Around Nozzle Exit	psfa
p_s	Static Pressure Inside Nozzle at the Exit	psfa
p_o	Total Pressure	psfa
p	Static Pressure	psfa
P_r	Prandtl Number	
R	Gas Constant for Air	53.35 feet/°R
T	Static Temperature	°R
T_{aw}	Adiabatic Wall Temperature	°R
T_o	Total Temperature	°R
$\dot{V}$	Velocity	feet/second
β	Ratio of Exit to Entrance Diameter of Nozzle	

γ	Ratio of Specific Heats (C_p/C_v)	
λ	Pressure Ratio (p_o/p_a)	
ρ	Mass Density	slugs/feet^3

SUBSCRIPTS

act	Actual
I	Ideal Based on Ambient Conditions
i	Ideal Based on Exit Static Conditions

LIST OF TABLES AND FIGURES

I. INTRODUCTION

This study, sponsored by the General Electric Company under their Purchase Order Number 200G230085, determined the discharge and velocity coefficients of an ASME long radius metering nozzle. Previous tests of this nozzle (Reference 1) had been conducted with an exhauster system which permitted operation at variable pressure ratio while keeping the Reynolds number constant. These additional tests were conducted to determine:

A. Whether the presence of the exhauster duct or the survey rake significantly affected the integrated data.

B. The effect of further changes of operating pressure ratio in the lower ranges of pressure ratio.

C. The effect of decreasing the Reynolds number.

II. CONCLUSIONS

A. These tests confirmed the observation made in the preceding test program (0431, Reference 1) that the core survey rake caused a consistent and appreciable increase in the measured static pressure, p_s , inside the nozzle near the exit. It may be concluded that this effect is present whether or not the exit plenum is installed. The effect is probably a manifestation of the sensitivity of transonic flow to small amounts of blockage, since the measured increase in pressure became greater as the pressure ratio approached the critical (choking) value.

B. The nozzle discharge coefficient showed an increasing trend with Reynolds number, varying from 0.989 at $Re = 10^6$ to 0.992 at $Re = 10^7$. The nozzle pressure ratio showed no consistent, independent effect on the discharge coefficient.

C. The nozzle thrust coefficient (at pressure ratios less than critical) also showed an increasing trend with Reynolds number, varying from 0.992 at $Re = 10^6$ to 0.995 at $Re = 6 \times 10^6$.

III. DISCUSSION

In the previous study conducted by FluiDyne, discharge and thrust coefficients were determined for a 7.715 inch diameter ASME long radius nozzle. The nozzle for these tests discharged into a cylindrical plenum in which pressure could be controlled by ejectors to vary the pressure ratio. The total pressure was held constant for most of the runs, giving a fairly constant throat Reynolds number.

For this test program, the metering nozzle discharged to atmosphere to eliminate any effects that might have been caused by the plenum on the first test series. Discharging to atmosphere meant that the nozzle pressure ratio and throat Reynolds number were controlled by the nozzle total pressure. Discharge and thrust coefficients were obtained over a pressure ratio range of 1.03 to 3.98 which corresponds to a Reynolds number variation of 0.95×10^6 to 12.0×10^6.

The nozzle instrumentation was the same as for the previous test program except that the total pressure cross-rake, used to survey the core flow at the exit of the nozzle, was only installed on four runs. These four runs were made to determine the effect of the cross-rake on the static pressure near the nozzle exit. Mercury and water manometers were used for all pressure measurements.

The data reduction procedures used for these data were the same as described in the report for Project 0431. The calculations and plots of the integrands of the discharge and thrust coefficient equations are shown in Figures 9 to 42. The tabulated test results are presented as Table I.

A plot of typical static pressure distributions through the nozzle is presented as Figure 2. A tabulation of these same typical static pressures is presented as Table II. The ratio of nozzle static to ambient pressure ($Ps/_{Pa}$) is plotted versus nozzle pressure ratio for each data point of the two test programs and presented in Figure 3. Both sets of data closely follow the ideal curve for pressure ratios greater than two. For pressure ratios less than two, the data points taken on the 0431 program and the data points with the exit cross-rake installed on the 0470 program have a $Ps/_{Pa}$ ratio slightly higher than the ideal curve. The ratio of $Ps/_{Pa}$ in this lower pressure ratio range is presented as an expanded portion of the curve as Figure 4.

The nozzle discharge coefficients plotted versus nozzle pressure ratio and Reynolds number are presented as Figures 5 and 6, respectively. The discharge coefficients obtained in the previous study are also presented in these plots. The discharge coefficients obtained in the two test programs agree when compared on a throat Reynolds number basis, as would be expected from similitude considerations.

The two sets of thrust coefficient data, plotted versus nozzle pressure ratio, are presented as Figure 7. The same thrust coefficient data, obtained at pressure ratios equal to or less than two, are plotted versus Reynolds number and presented as Figure 8. Good agreement is obtained between these two sets of data when compared at like pressure ratios. Good agreement is also obtained when compared on a Reynolds number basis.

Reference 1. "Determination of Discharge and Thrust Coefficients of a Choked ASME Nozzle from Exit Flow Surveys," James S. Holdhusen and Charles L. Landgraf, FluiDyne Project 0431, February 1965.

TABLE 1 TABULATED TEST RESULTS

Data Point	Press. Ratio	Po (psia)	Ps (psia)	Pa (psia)	Ps/Pa	$\int \frac{M}{M_I}\sqrt{\frac{T_I}{T}}\ \frac{dA}{A_E}$	$\int \left(\frac{M}{M_I}\right)^2 \frac{dA}{A_E}$	C_D	C_V	Cs	Thrt. Re x 10^{-6}
1	1.209	17.23	14.29	14.25	1.0031	.9902	.9829	.9902	.9927	1.1541	2.54
2	2.408	35.20	18.21	14.25	1.2779	.9923	.9874	.9923	.9952	1.2689	7.47
3	1.418	20.14	14.28	14.21	1.0052	.9905	.9840	.9905	.9953	1.2248	3.62
4	1.643	23.34	14.32	14.21	1.0079	.9905	.9851	.9905	.9948	1.2592	4.66
5	1.857	26.37	14.45	14.21	1.0176	.9915	.9865	.9915	.9952	1.2683	5.60
6	2.059	29.25	15.41	14.21	1.0848	.9921	.9869	.9921	.9953	1.2682	6.19
8	2.276	32.23	16.79	14.42	1.1860	.9924	.9879	.9924	.9968	1.2704	6.83
9	2.487	35.21	18.35	14.42	1.2959	.9925	.9880	.9925	.9953	1.2680	7.47
10	2.710	38.37	20.02	14.42	1.4141	.9925	.9876	.9925	.9941	1.2683	8.15
11	2.904	41.05	21.27	14.14	1.5052	.9923	.9878	.9923	.9918	1.2683	8.70
12	3.120	44.09	22.88	14.13	1.6193	.9925	.9880	.9925	.9888	1.2704	9.44
13	3.355	47.20	24.57	14.05	1.7491	.9925	.9883	.9925	.9880	1.2686	10.0
14	3.568	50.10	26.11	14.04	1.8602	.9924	.9880	.9924	.9875	1.2678	10.6
15	3.773	52.96	27.60	14.04	1.9662	.9926	.9880	.9926	.9838	1.2681	11.2
16a	3.985	55.93	29.27	14.03	2.0854	.9930	.9885	.9930	.9819	1.2683	12.0
16b	3.929	55.13	28.79	14.03	2.0513	.9924	.9878	.9924	.9829	1.2683	11.9
17	1.219	17.12	14.07	14.04	1.0021	.9903	.9836	.9903	.9929	1.1593	2.52
18	1.431	20.09	14.10	14.04	1.0045	.9911	.9853	.9911	.9938	1.2283	3.62
19	1.647	23.13	14.13	14.04	1.0066	.9912	.9855	.9912	.9939	1.2592	4.60
20	1.613	23.14	14.13	14.04	1.0063	.9903	.9840	.9903	.9936	1.2587	4.60
21	1.859	26.10	14.28	14.04	1.0171	.9917	.9870	.9917	.9954	1.2684	5.54
22	2.066	29.00	15.25	14.04	1.0861	.9922	.9876	.9922	.9937	1.2683	6.15
23	2.073	29.11	15.27	14.04	1.0875	.9923	.9876	.9923	.9957	1.2711	6.17
24	1.213	17.10	14.14	14.09	1.0035	.9908	.9843	.9908	.9939	1.1554	2.53
25	1.647	23.21	14.48	14.09	1.0278	.9918	.9864	.9918	.9950	1.2557	4.62
26	2.498	35.20	18.85	14.09	1.3373	.9928	.9879	.9928	.9953	1.2681	7.49
27	2.488	35.07	18.81	14.09	1.3348	.9925	.9878	.9925	.9955	1.2684	7.43
28	3.128	44.13	22.94	14.11	1.6260	.9927	.9882	.9927	.9895	1.2681	4.51
29	3.136	44.24	23.02	14.11	1.6319	.9928	.9882	.9928	.9903	1.2679	9.72
2-1	1.032	14.685	14.228	14.227	1.00007	.9893	.9815	.9893	.9921	1.0402	0.94
2-2	1.053	14.980	14.229	14.227	1.00010	.9900	.9818	.9900	.9917	1.0571	1.25
2-3	1.106	15.738	14.229	14.227	1.00012	.9898	.9818	.9898	.9919	1.0968	1.73
2-4	1.152	16.397	14.231	14.227	1.00027	.9897	.9827	.9897	.9929	1.1261	2.11
2-5	1.202	17.099	14.232	14.227	1.00033	.9900	.9835	.9900	.9934	1.1523	2.42

TABLE II

DIMENSIONLESS STATIC PRESSURE DISTRIBUTIONS

(P/Po)

Run Number	Press. Ratio λ = Po/Pa	Pa/Po $1/\lambda$	Values of P/Po — Tap Numbers 1-4*	5	6	7	8	9	10	11	12
1	1.209	.8271	.8295	.8310	.8324	.8310	.8239	.8197	.8182	.8011	.8410
3	1.418	.7052	.7088	.7125	.7161	.7125	.7003	.6930	.6930	.7015	.7477
4	1.643	.6086	.6135	.6169	.6232	.6211	.6065	.5971	.5950	.6191	.6943
5	1.857	.5385	.5481	.5609	.5702	.5729	.5609	.5488	.5479	.5896	.6787
6	2.059	.4857	.5269	.5477	.5611	.5661	.5544	.5419	.5419	.5879	.6791
8	2.276	.4394	.5212	.5473	.5587	.5632	.5518	.5397	.5397	.5860	.6764
9	2.487	.4021	.5211	.5453	.5599	.5641	.5522	.5404	.5404	.5863	.6780
11	2.904	.3444	.5184	.5441	.5572	.5626	.5501	.5382	.5388	.5853	.6783
14	3.568	.2803	.5213	.5445	.5582	.5636	.5504	.5387	.5387	.5856	.6774
16b	3.929	.2545	.5222	.5453	.5591	.5640	.5502	.5391	.5387	.5857	.6794

*Average

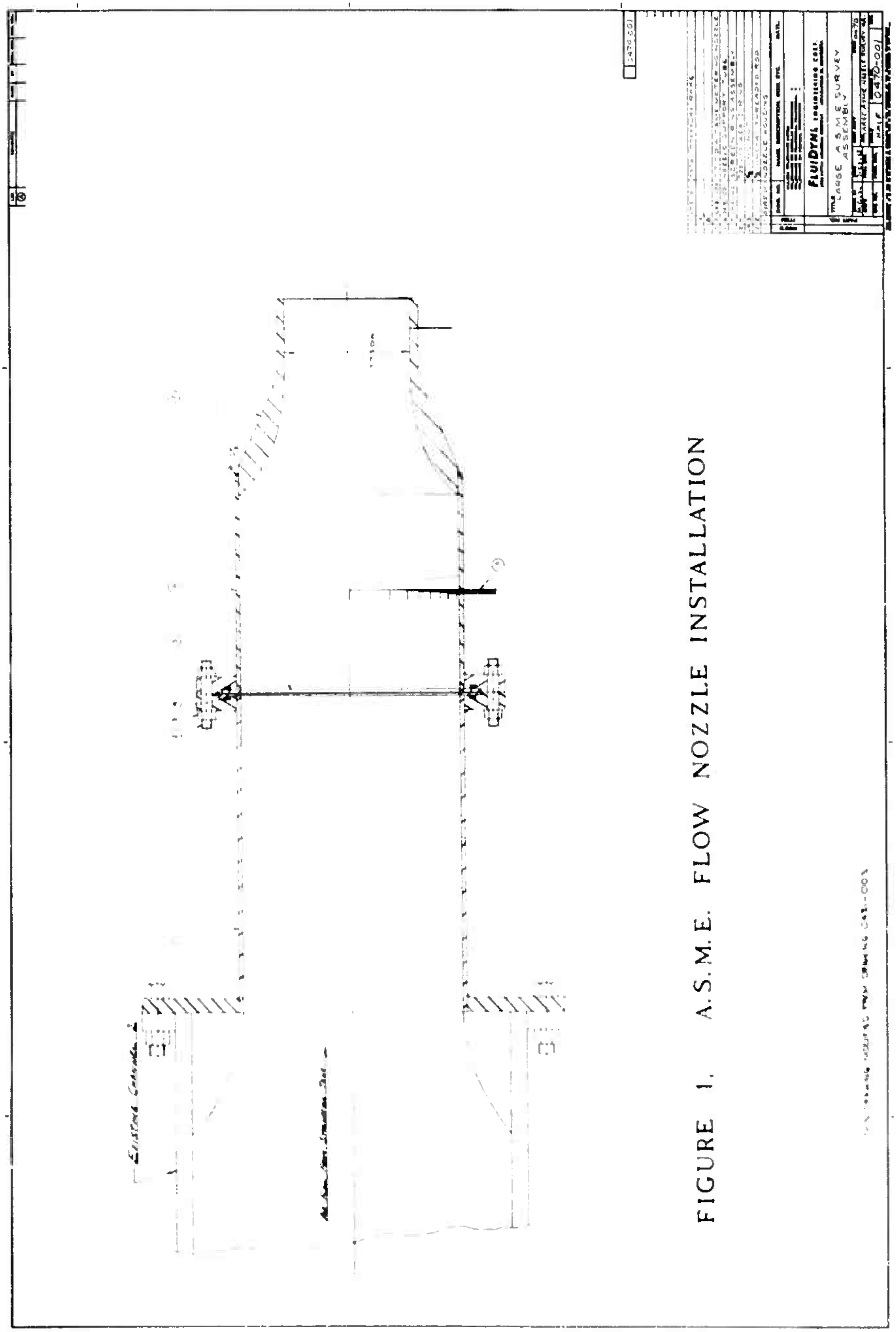

FIGURE 1. A.S.M.E. FLOW NOZZLE INSTALLATION

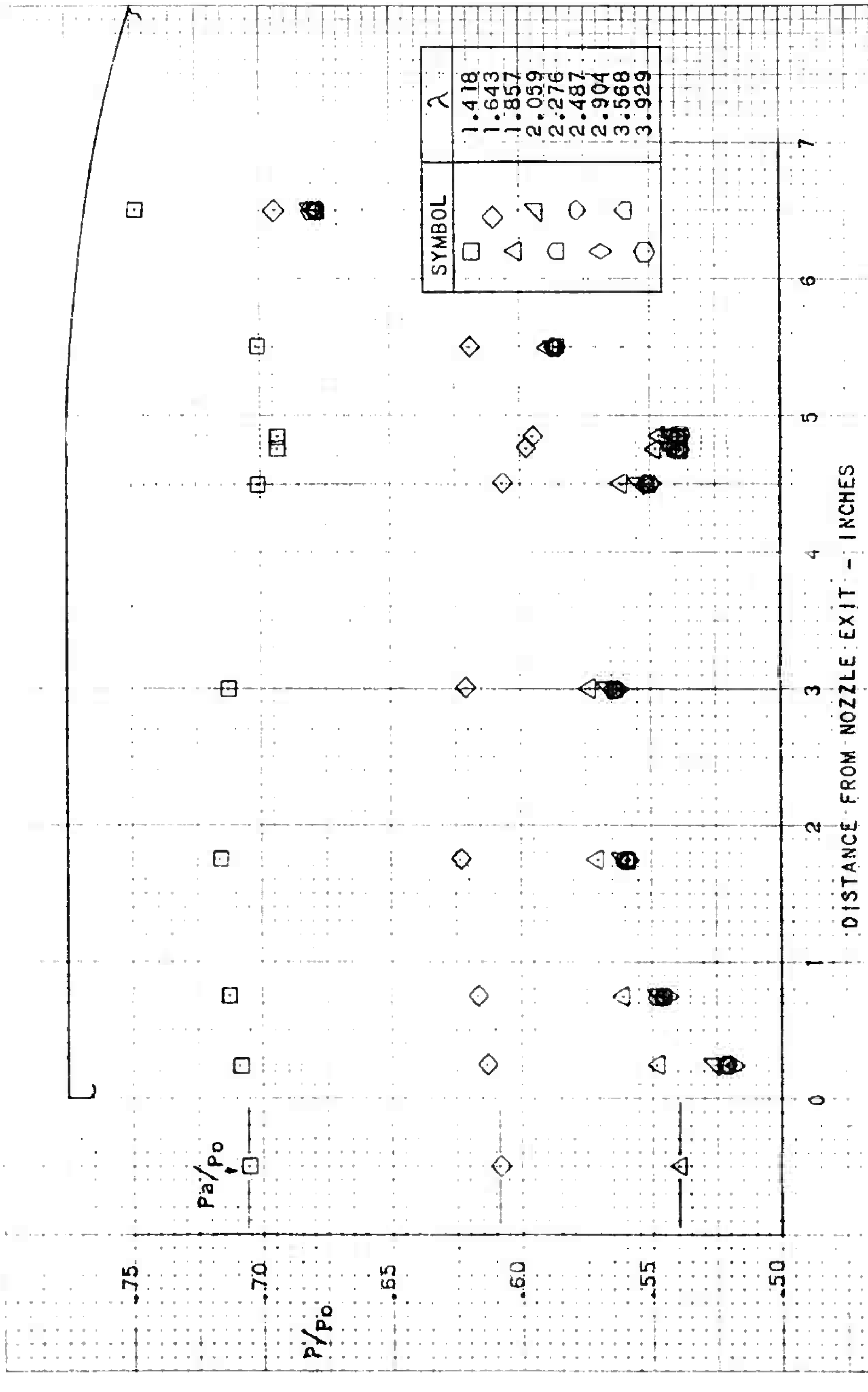

FIGURE 2. STATIC PRESSURE DISTRIBUTIONS

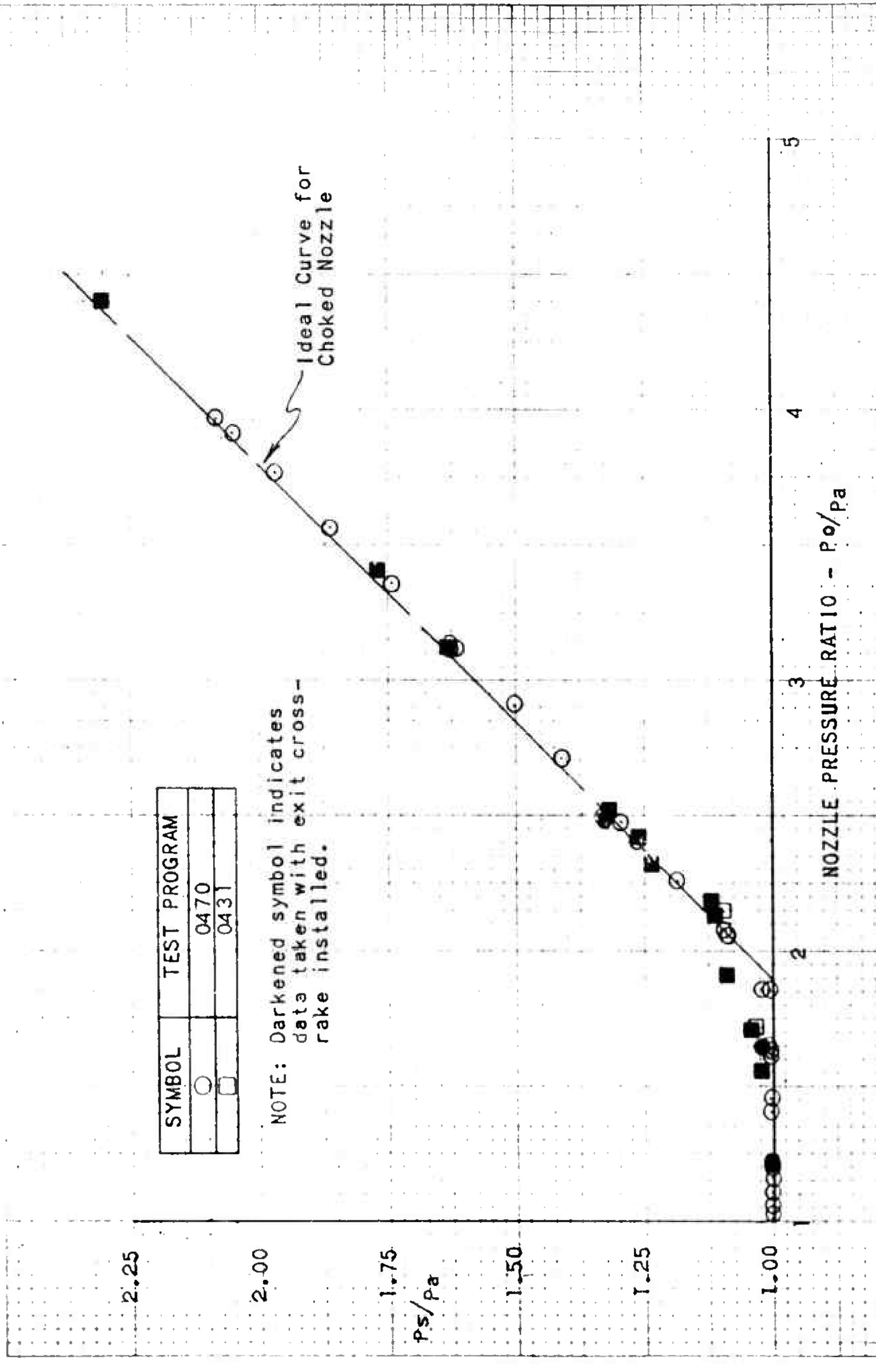

FIGURE 3. RATIO OF NOZZLE STATIC TO AMBIENT PRESSURE

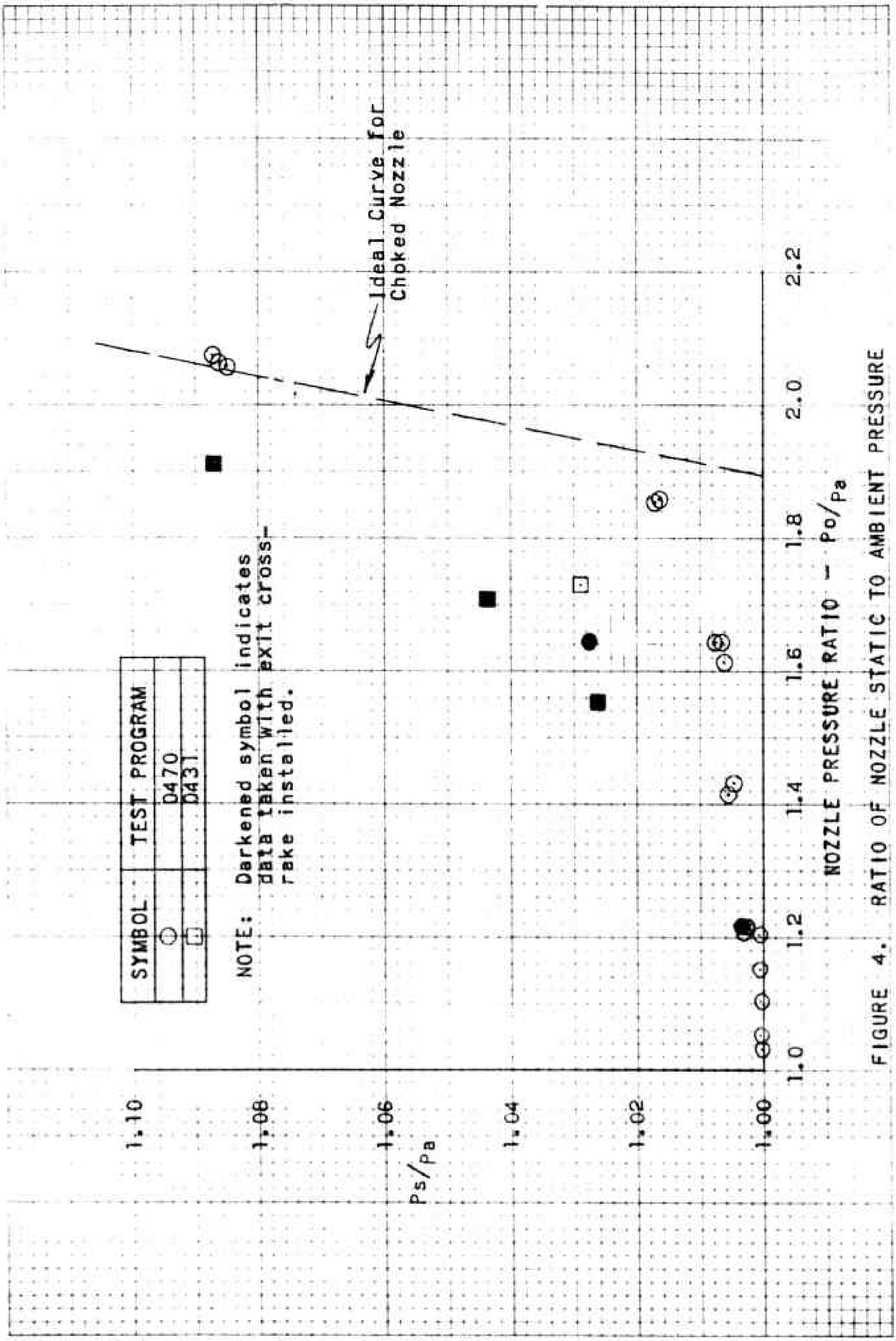

FIGURE 4. RATIO OF NOZZLE STATIC TO AMBIENT PRESSURE

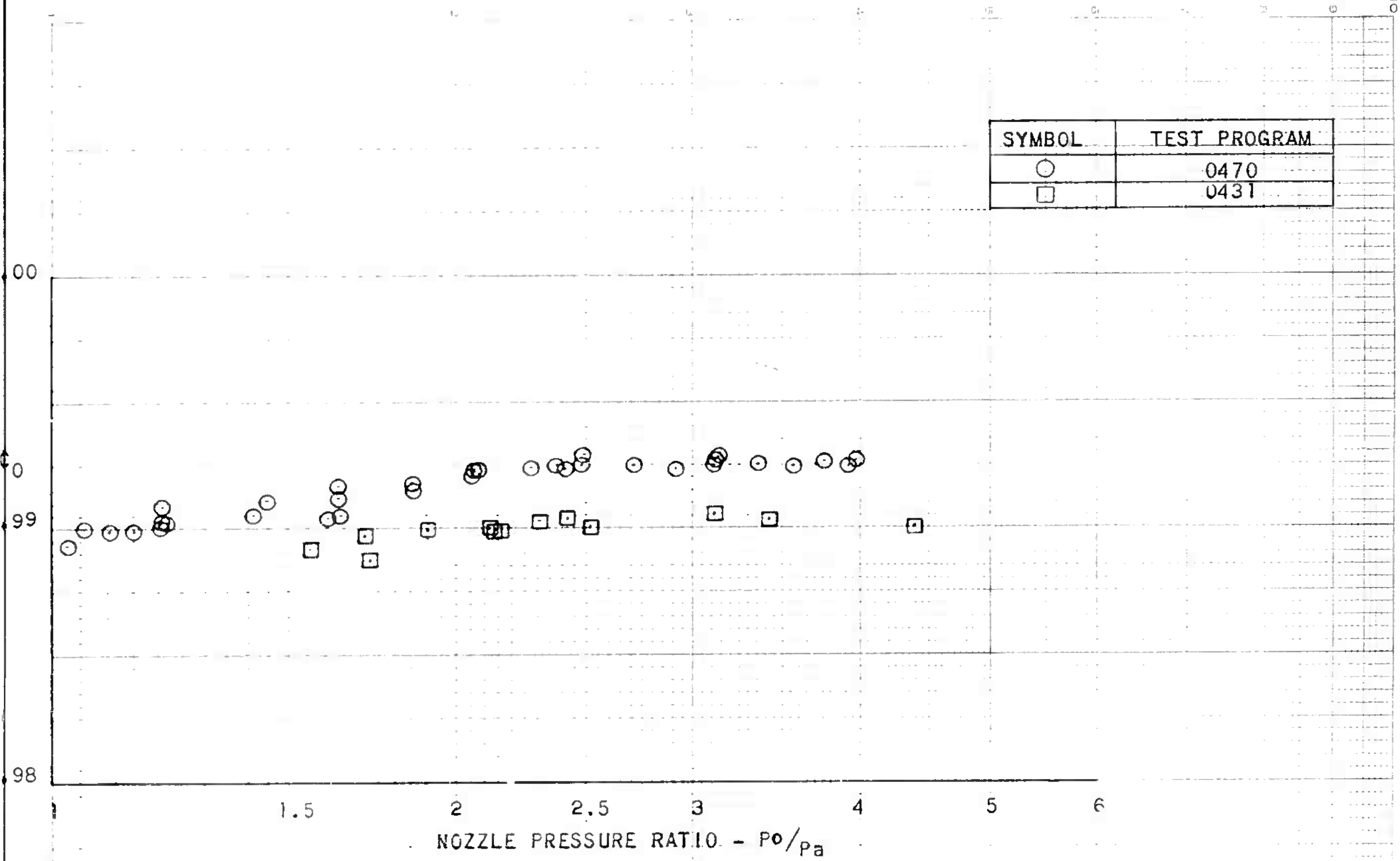

FIGURE 5. DISCHARGE COEFFICIENT VERSUS NOZZLE PRESSURE RATIO

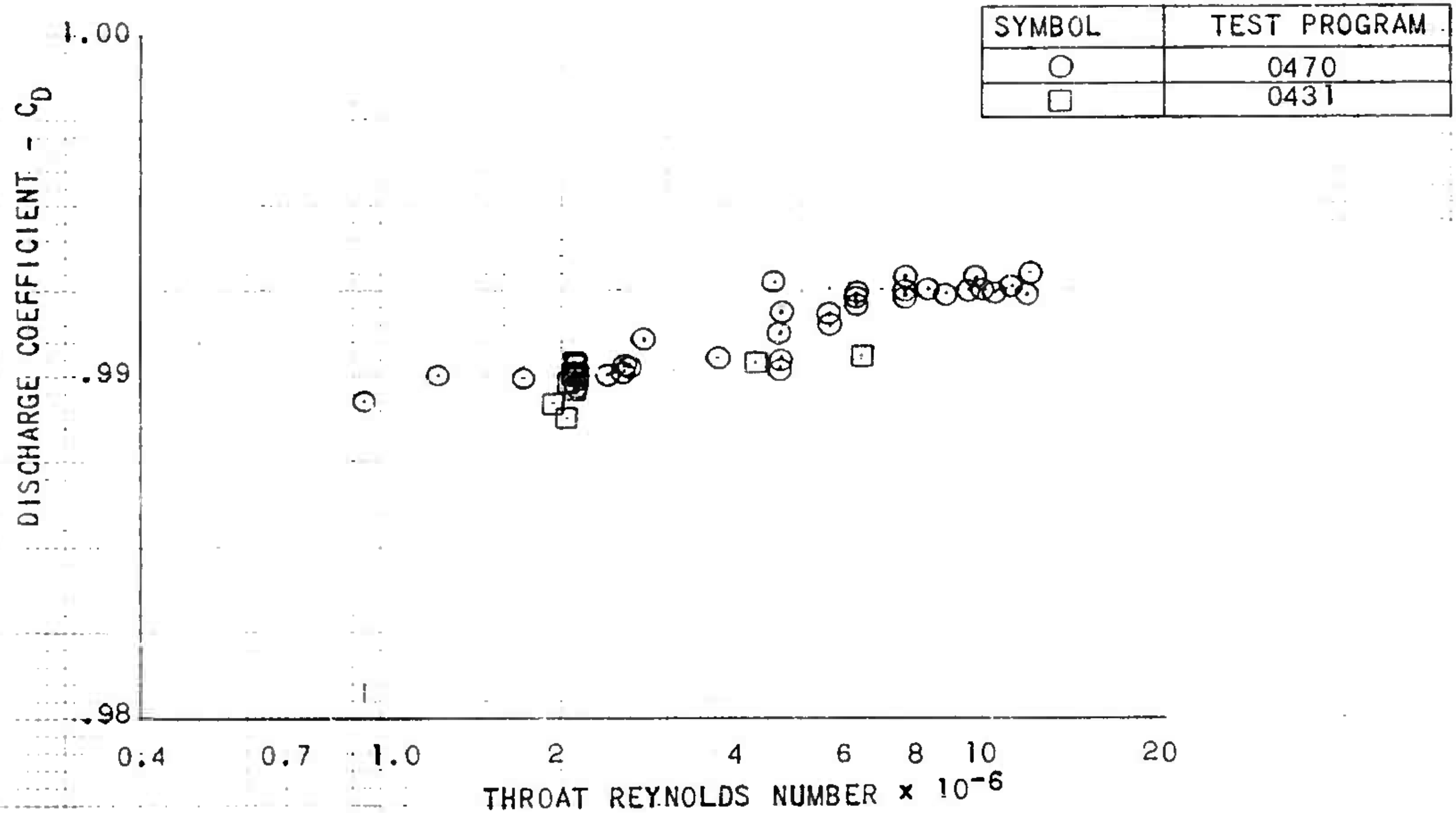

FIGURE 6. DISCHARGE COEFFICIENT VERSUS THROAT REYNOLDS NUMBER

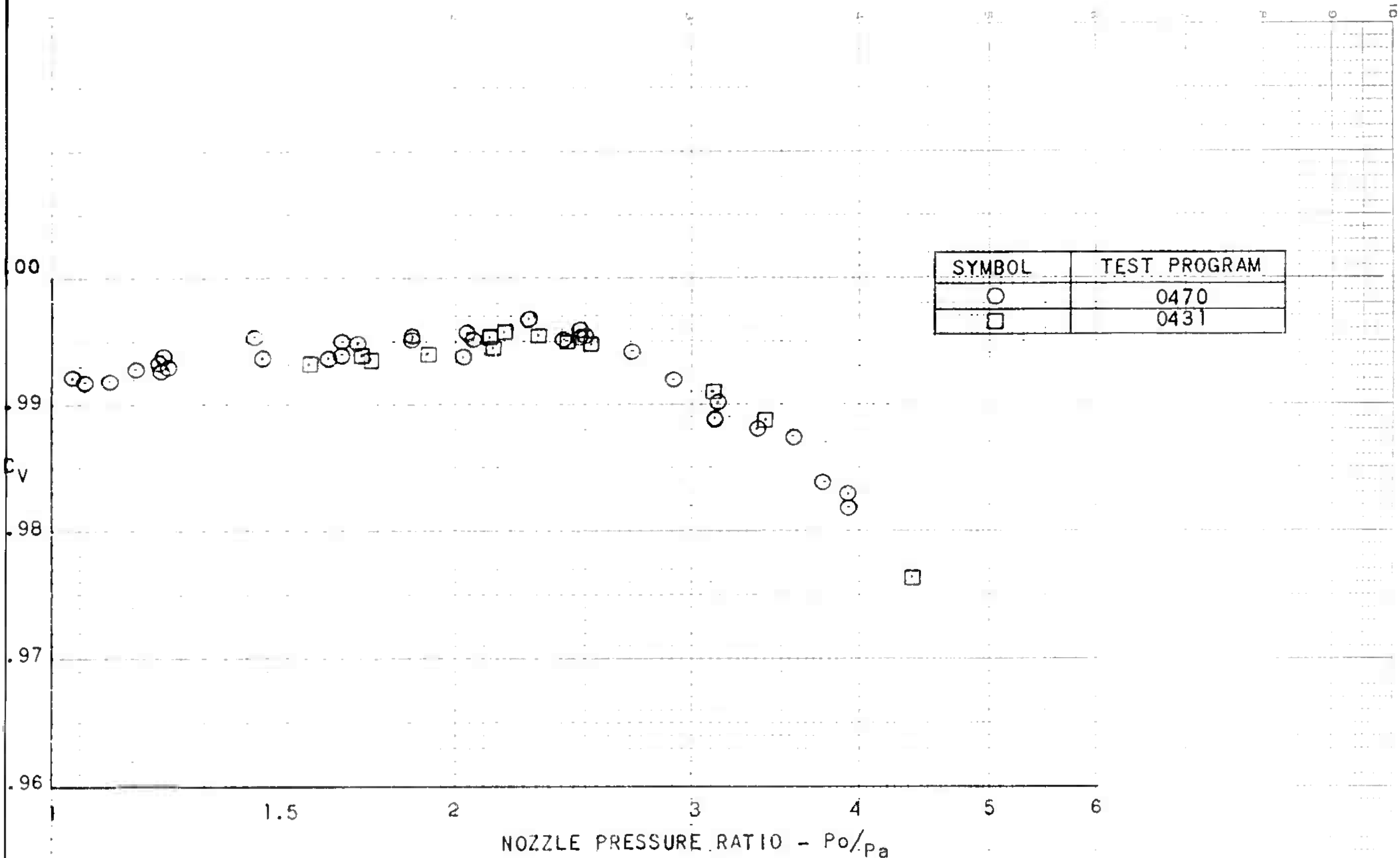

FIGURE 7. THRUST COEFFICIENT VERSUS NOZZLE PRESSURE RATIO

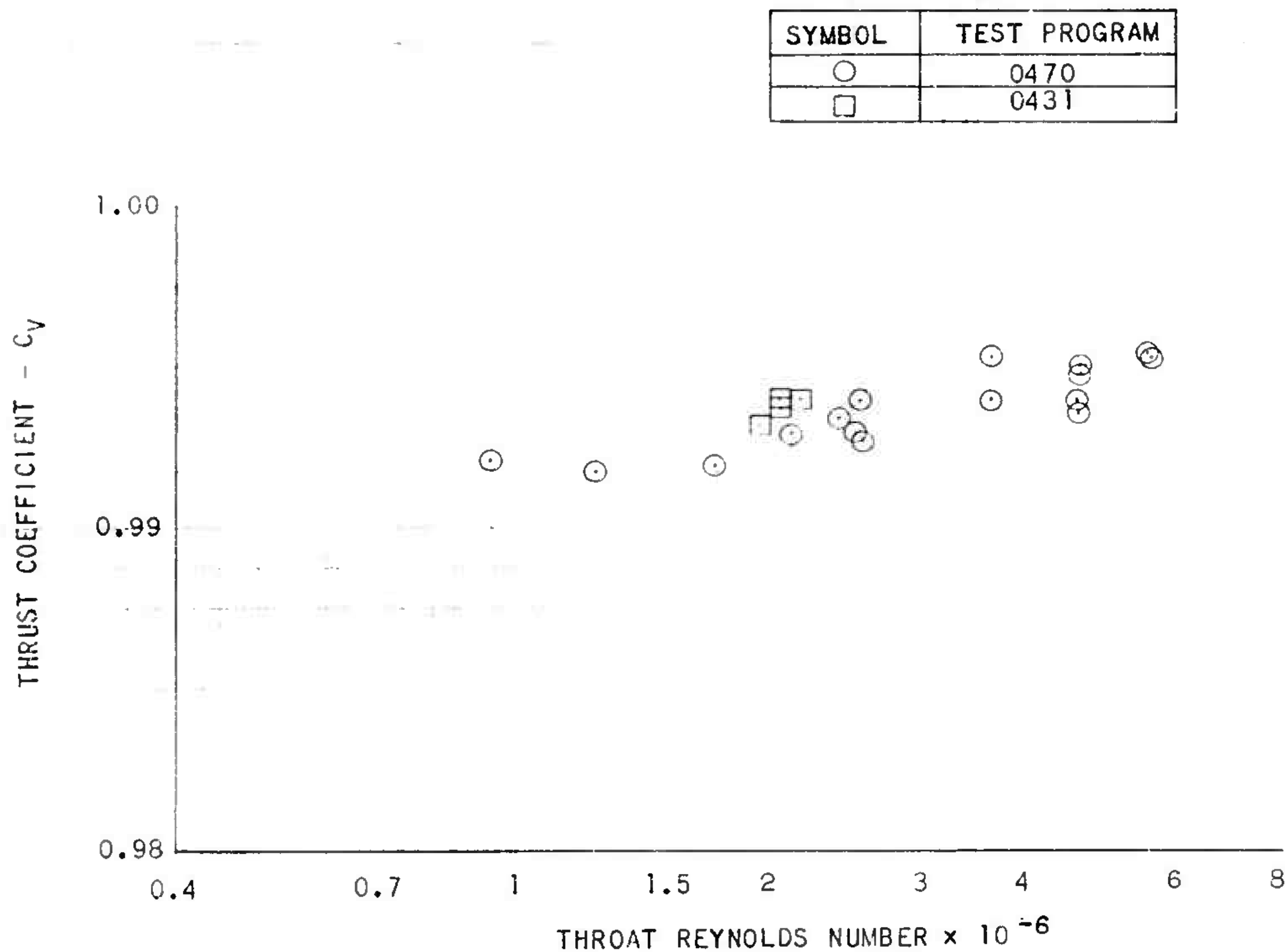

FIGURE 8. THRUST COEFFICIENT VERSUS THROAT REYNOLDS NUMBER

FLUIDYNE ENGINEERING CORPORATION

INTEGRATION CURVES

TO DETERMINE C_D & C_V

RUN 2 DATA POINT 2.4706

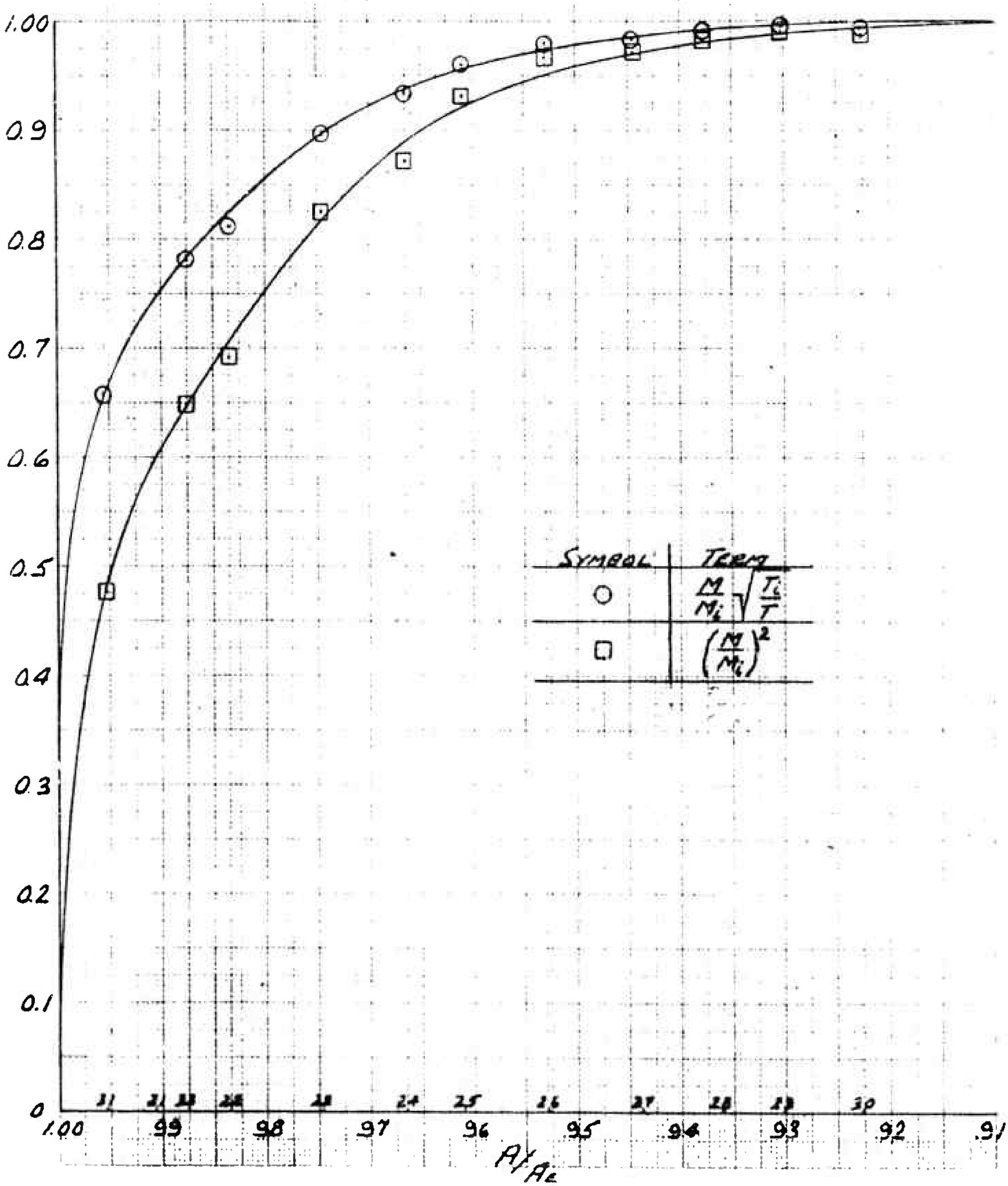

SYMBOL	TERM
○	$\frac{M}{M_i}\sqrt{\frac{T_i}{T}}$
□	$\left(\frac{M}{M_i}\right)^2$

FLUIDYNE ENGINEERING CORPORATION

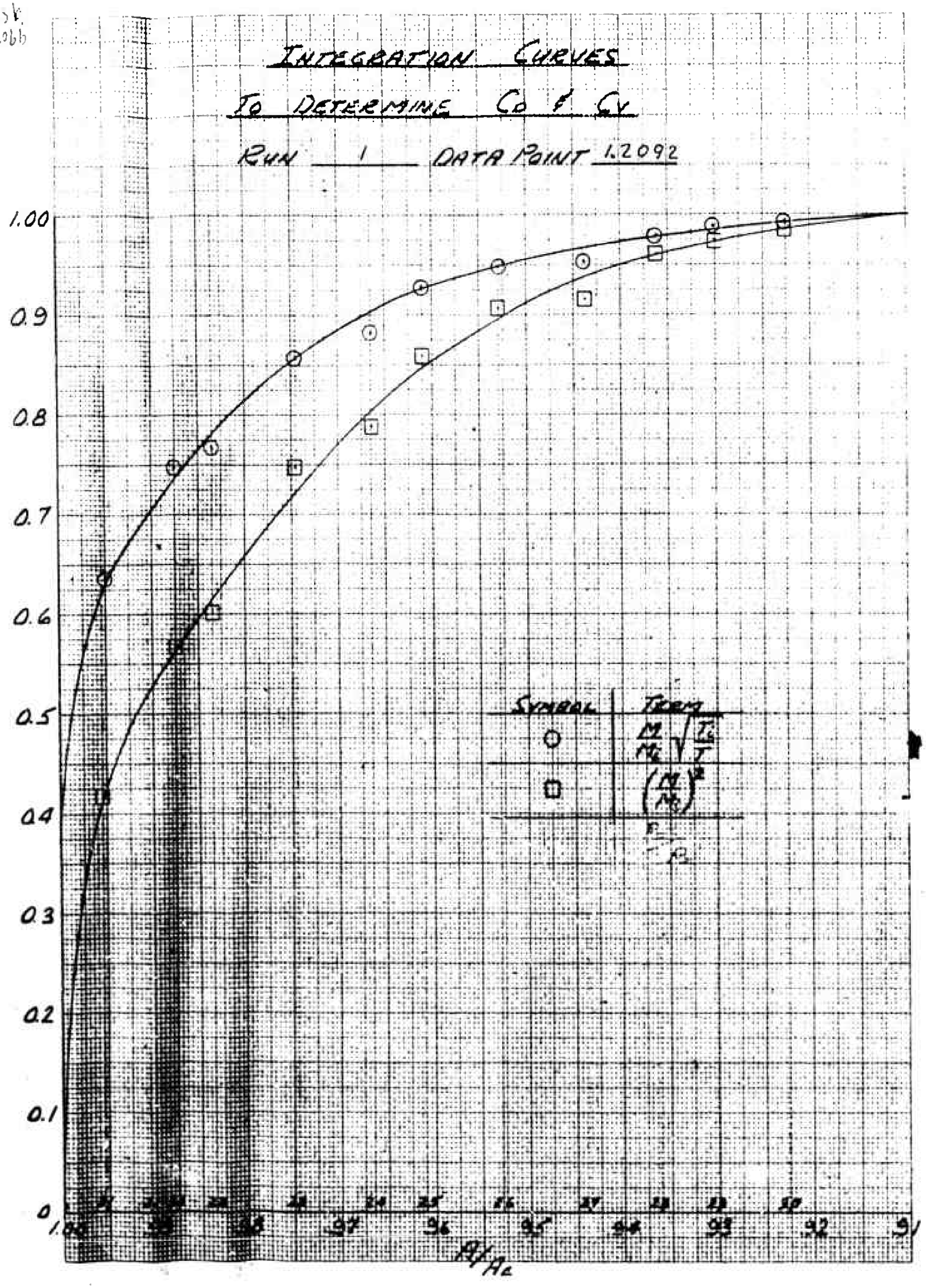

0486
5066

FLUIDYNE ENGINEERING CORPORATION

INTEGRATION CURVES
TO DETERMINE C_D & C_V
RUN 3 DATA POINT 1.4180

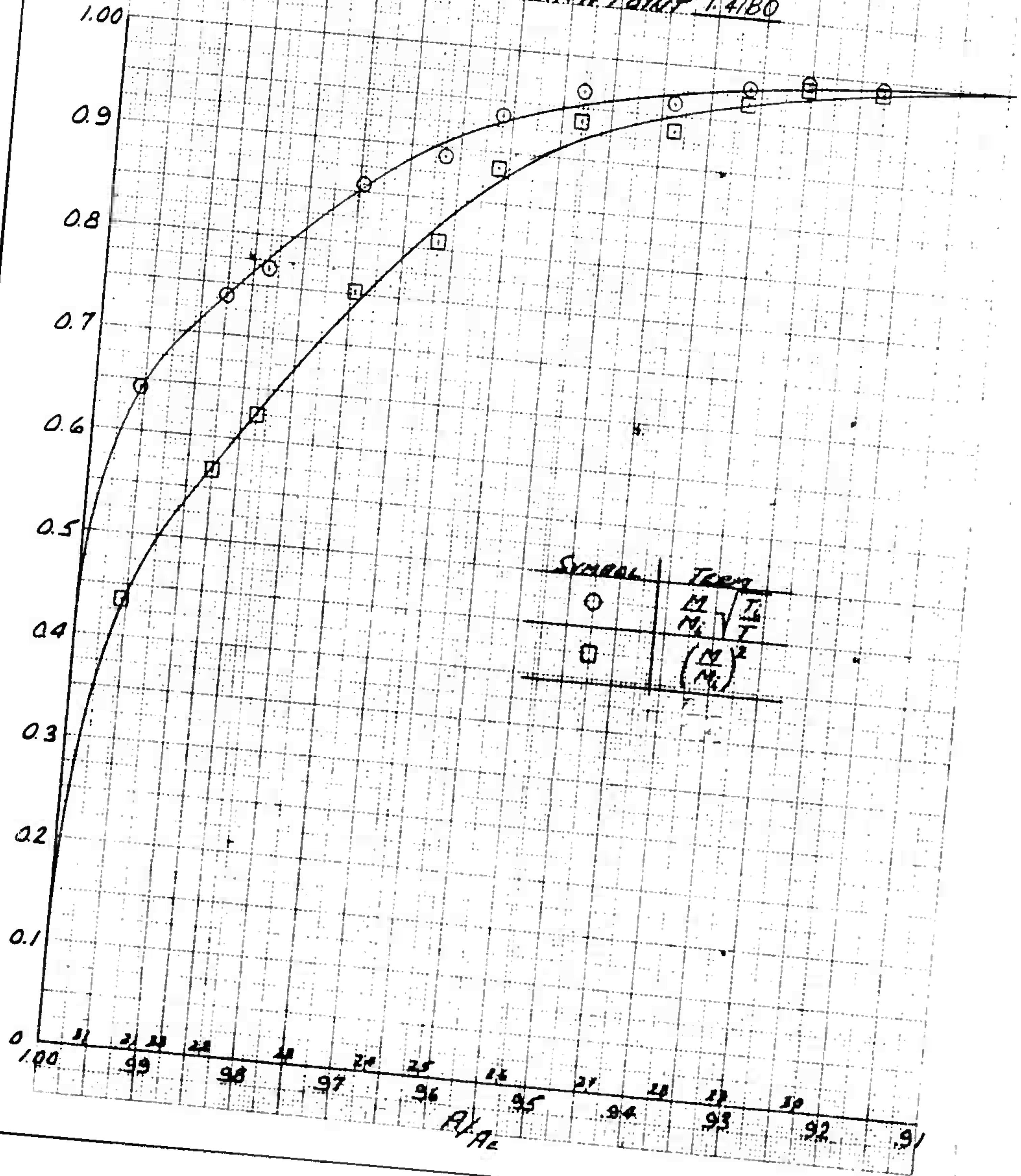

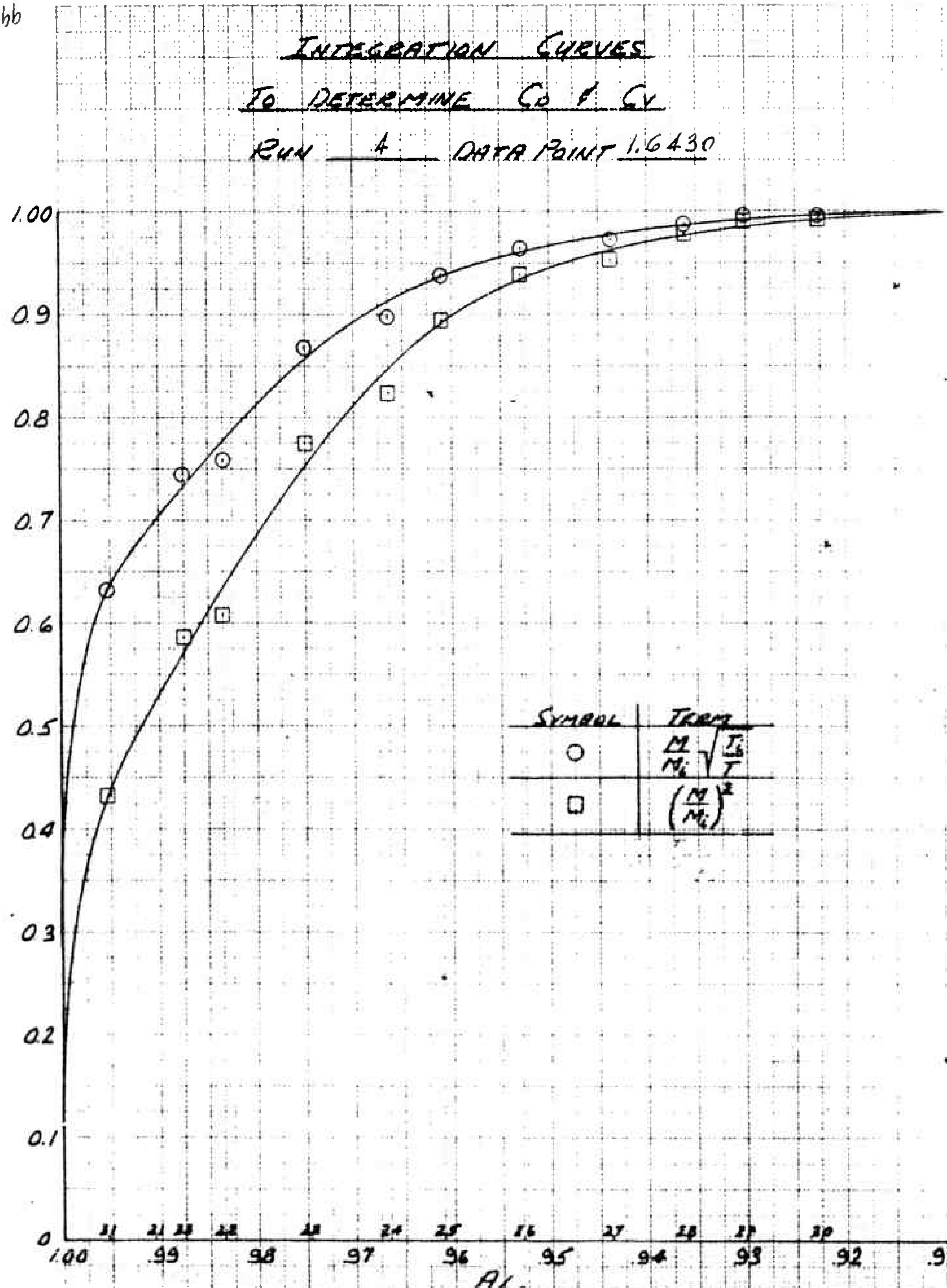

INTEGRATION CURVES
TO DETERMINE CD & CV
RUN 4 DATA POINT 1.6430
1.00
0.9
0.8
0.7
0.6
0.5
0.4
0.3
0.2
0.1
0
1.00
.99
.98
.97
.96
.95
.94
.93
.92
.91
A/Ac
SYMBOL
TERM
$\frac{M}{M_i}\sqrt{\frac{T_i}{T}}$
$\left(\frac{M}{M_i}\right)^2$

INTEGRATION CURVES

TO DETERMINE C_D & C_V

RUN 5 DATA POINT 1.8567

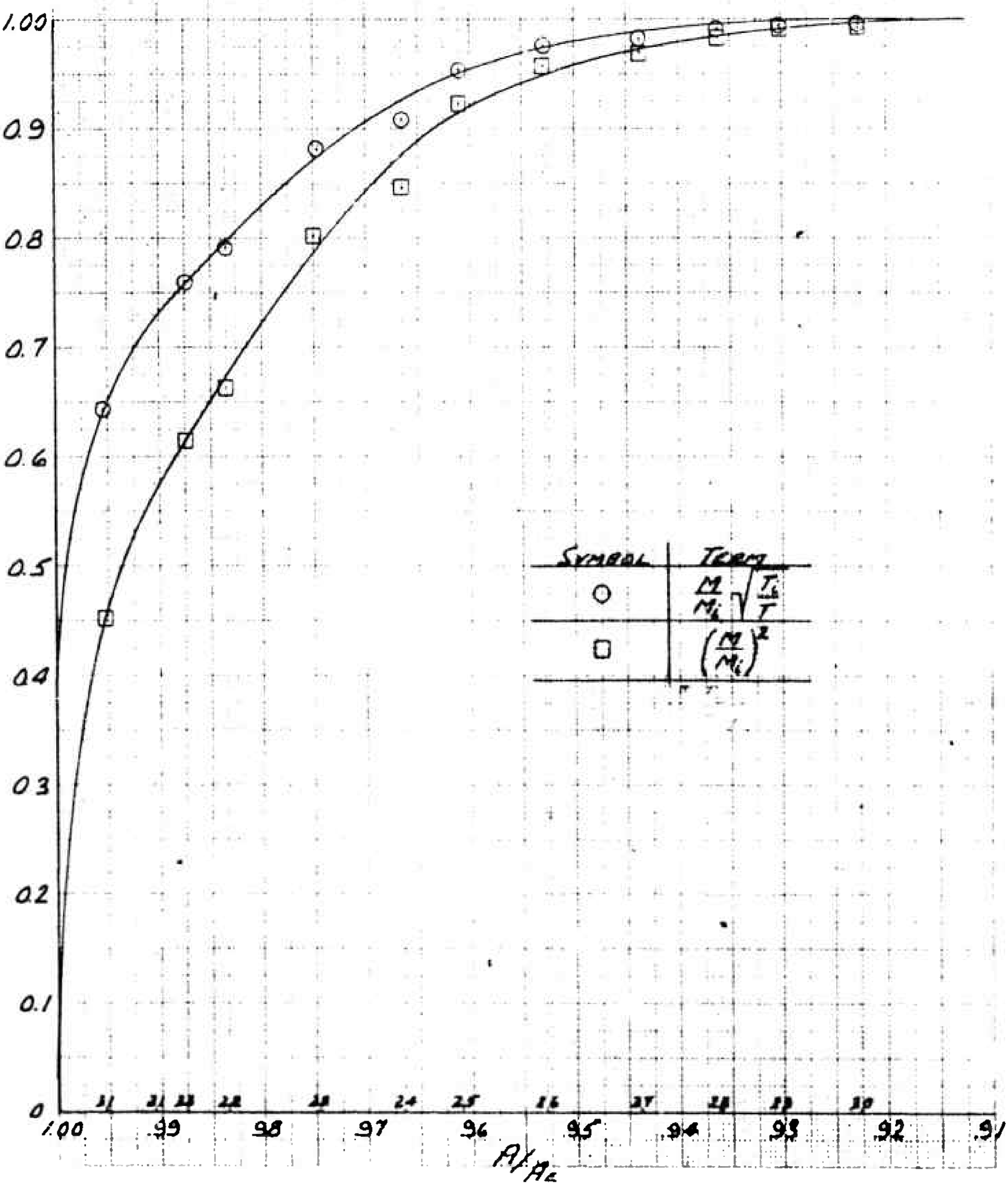

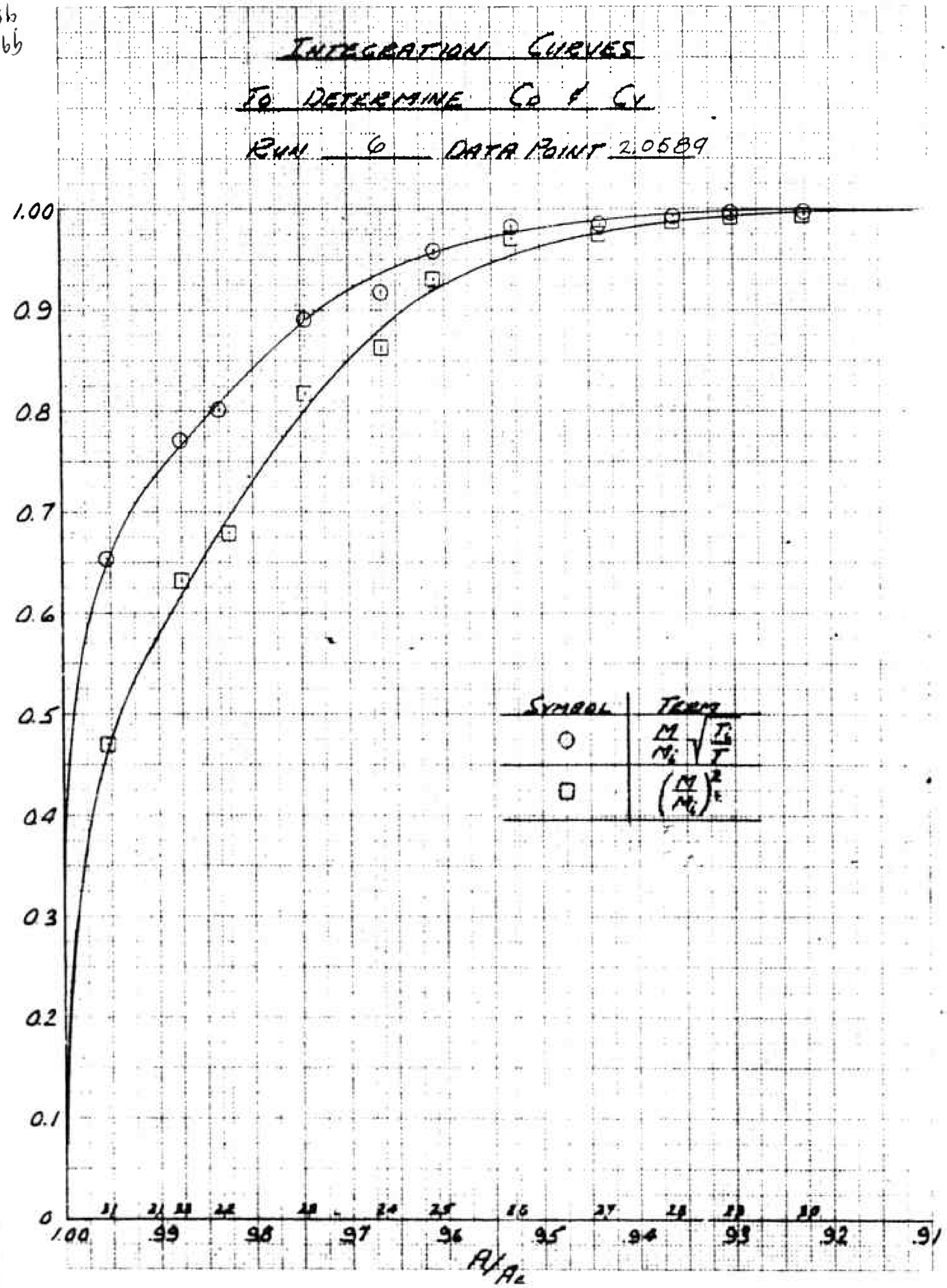
INTEGRATION CURVES
TO DETERMINE C_D & C_V
RUN 6 DATA POINT 2.0589
1.00
0.9
0.8
0.7
0.6
0.5
0.4
0.3
0.2
0.1
0
1.00
.99
.98
.97
.96
.95
.94
.93
.92
.91
A/Ai
SYMBOL
TERM

FLUIDYNE ENGINEERING CORPORATION

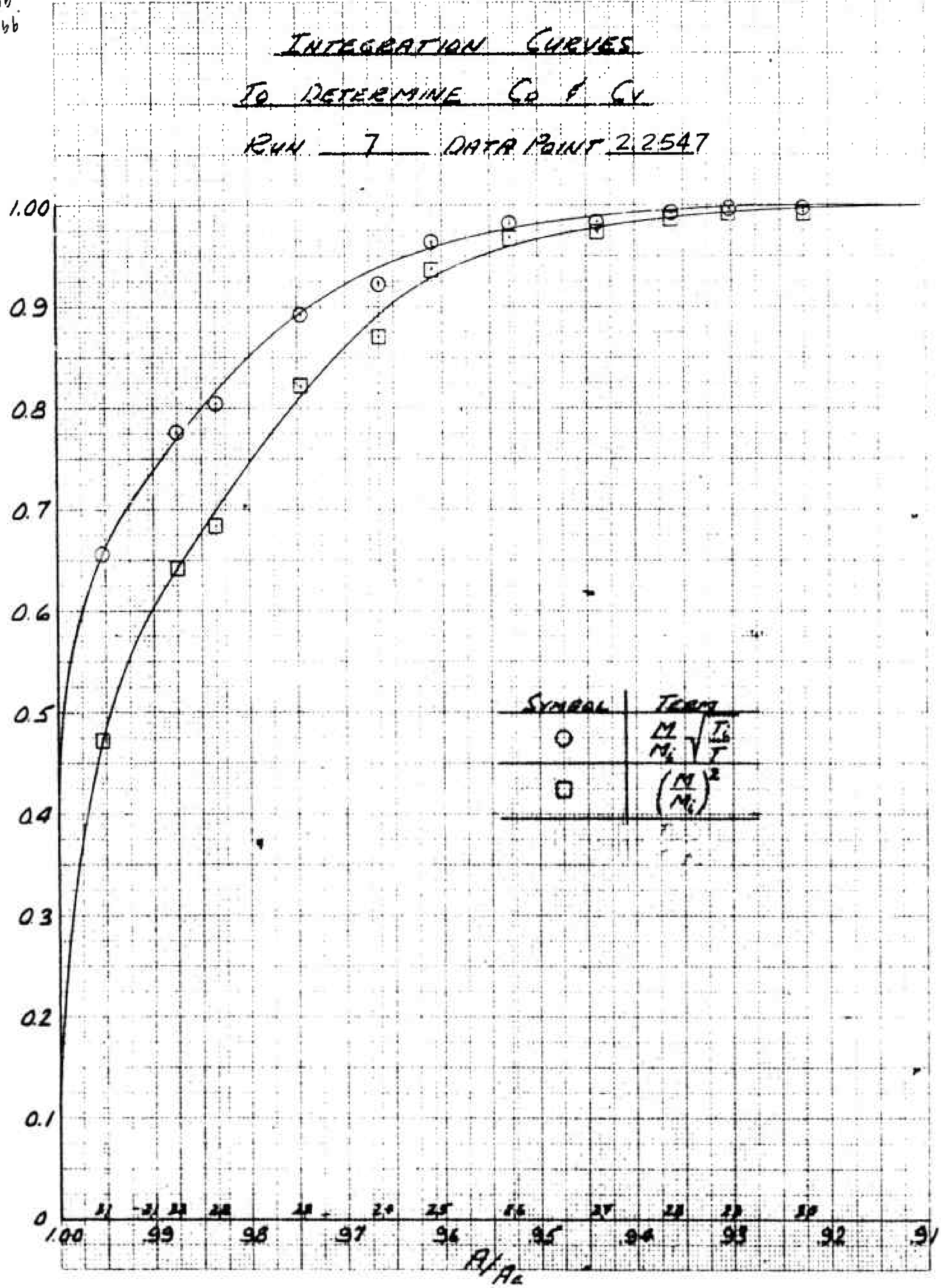

FluiDyne Engineering Corporation

Integration Curves

To Determine C_D & C_V

Run 8 Data Point 2.2762

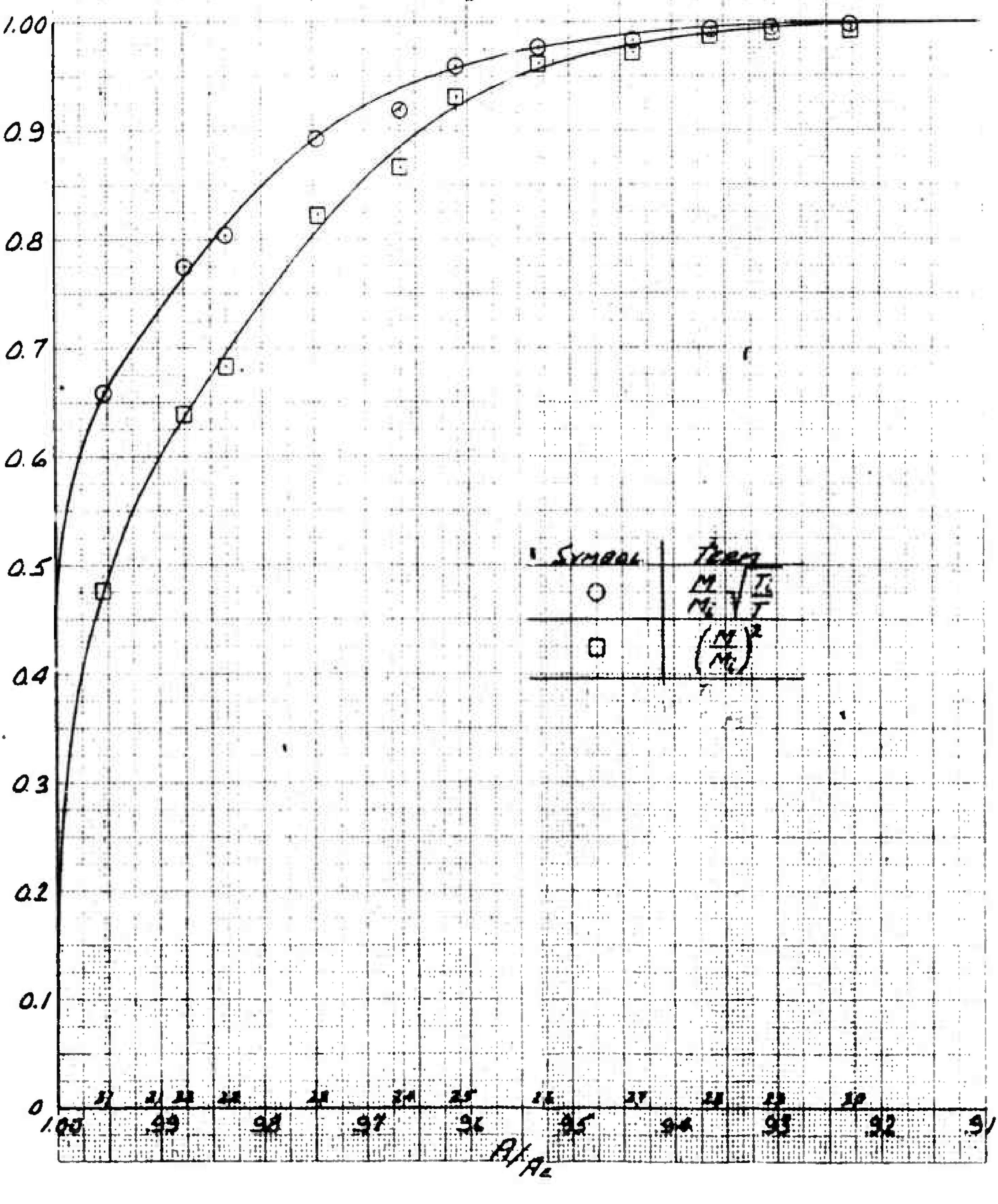

c336
3266

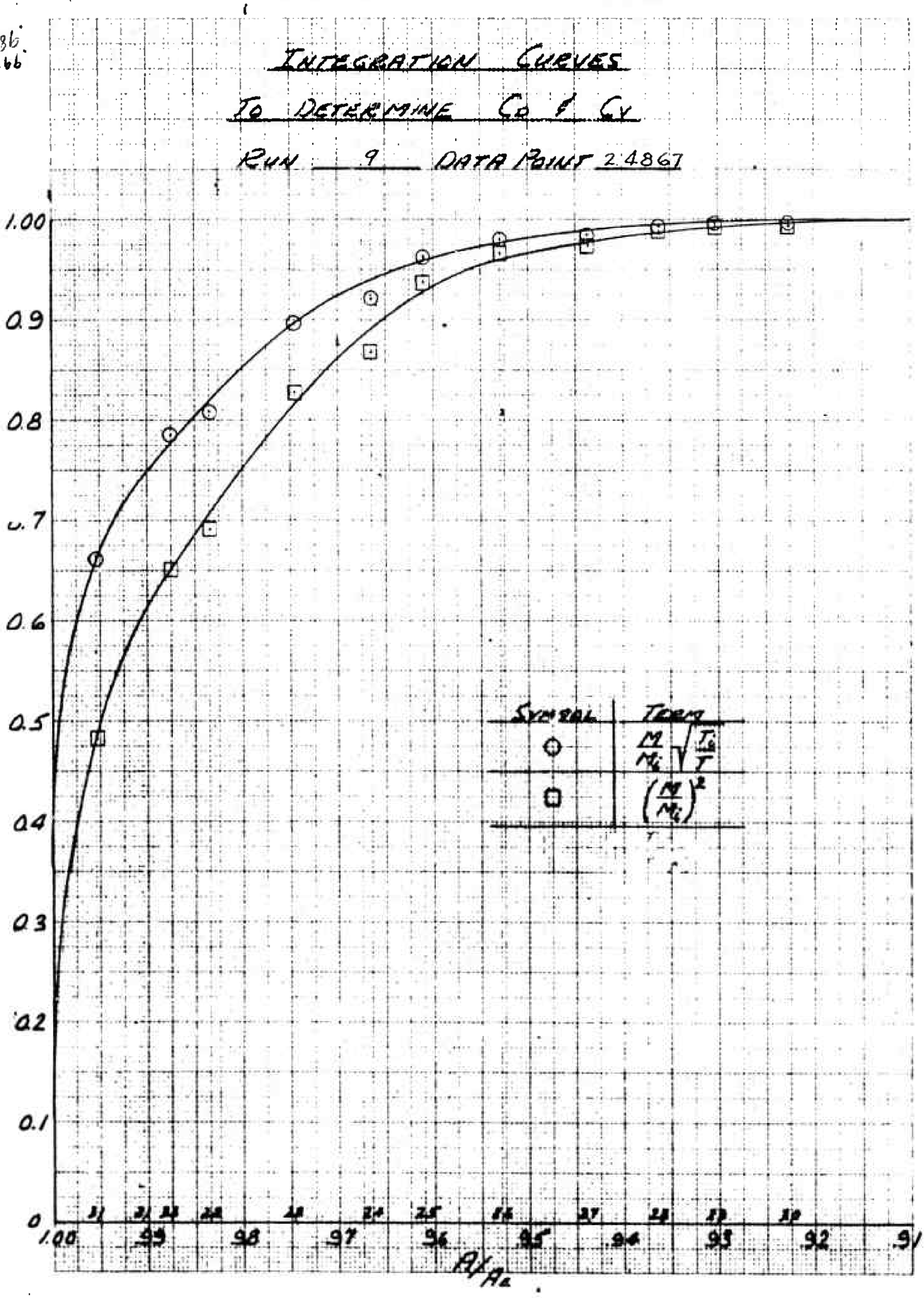
INTEGRATION CURVES
TO DETERMINE C_D & C_V
RUN 9 DATA POINT 2.4867
1.00
0.9
0.8
0.7
0.6
0.5
0.4
0.3
0.2
0.1
0
SYMBOL
TERM
$\frac{M}{M_i}\sqrt{\frac{T_0}{T}}$
$\left(\frac{M}{M_i}\right)^2$
1.00
.99
.98
.97
.96
.95
.94
.93
.92
.91
A/A_2

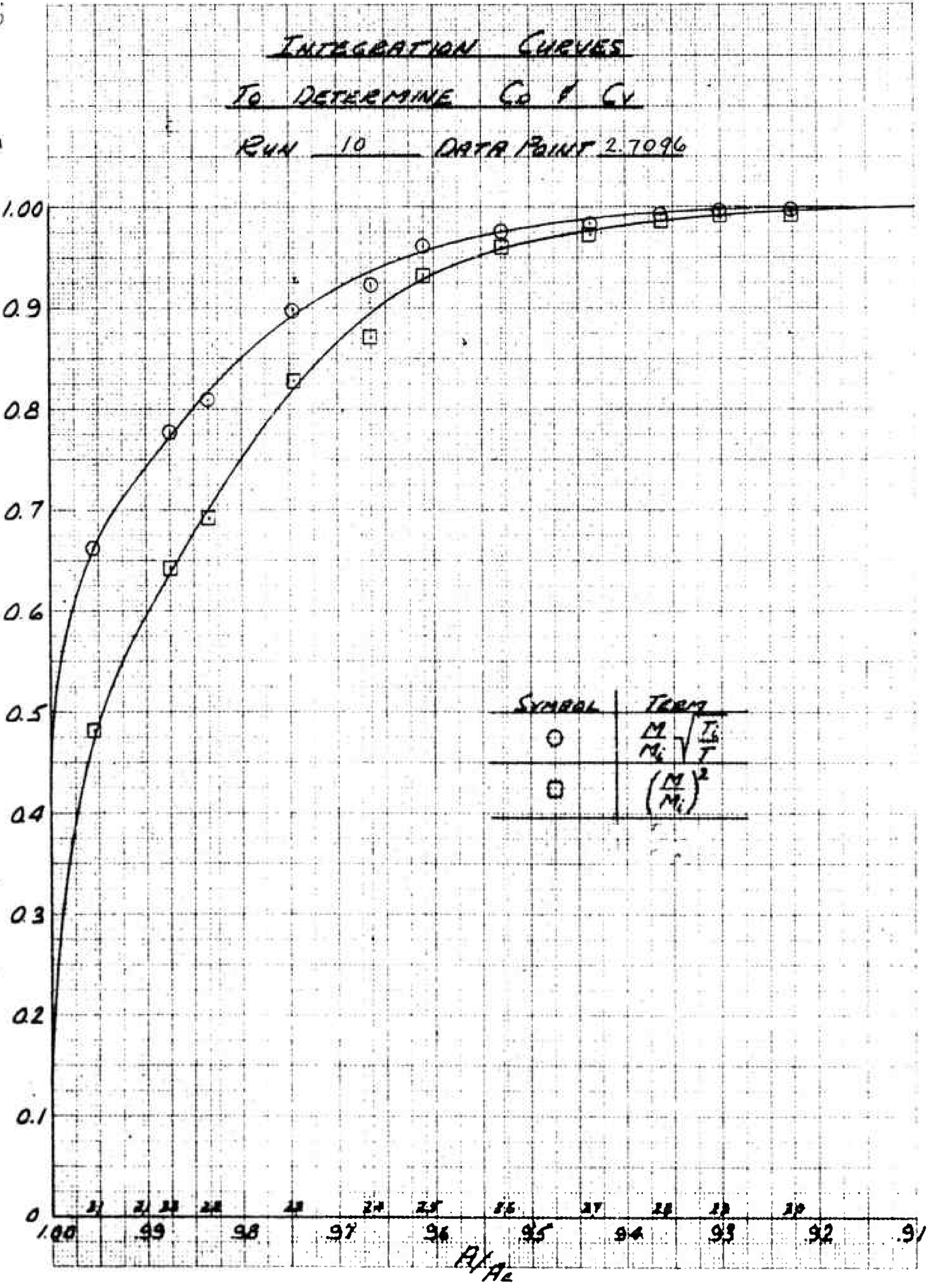
INTEGRATION CURVES
TO DETERMINE CD & CV
RUN 10 DATA POINT 2.7096
1.00
0.9
0.8
0.7
0.6
0.5
0.4
0.3
0.2
0.1
0
SYMBOL
TERM
$\frac{M}{M_i}\sqrt{\frac{T_i}{T}}$
$\left(\frac{M}{M_i}\right)^2$
1.00
.99
.98
.97
.96
.95
.94
.93
.92
.91
A_x/A_c

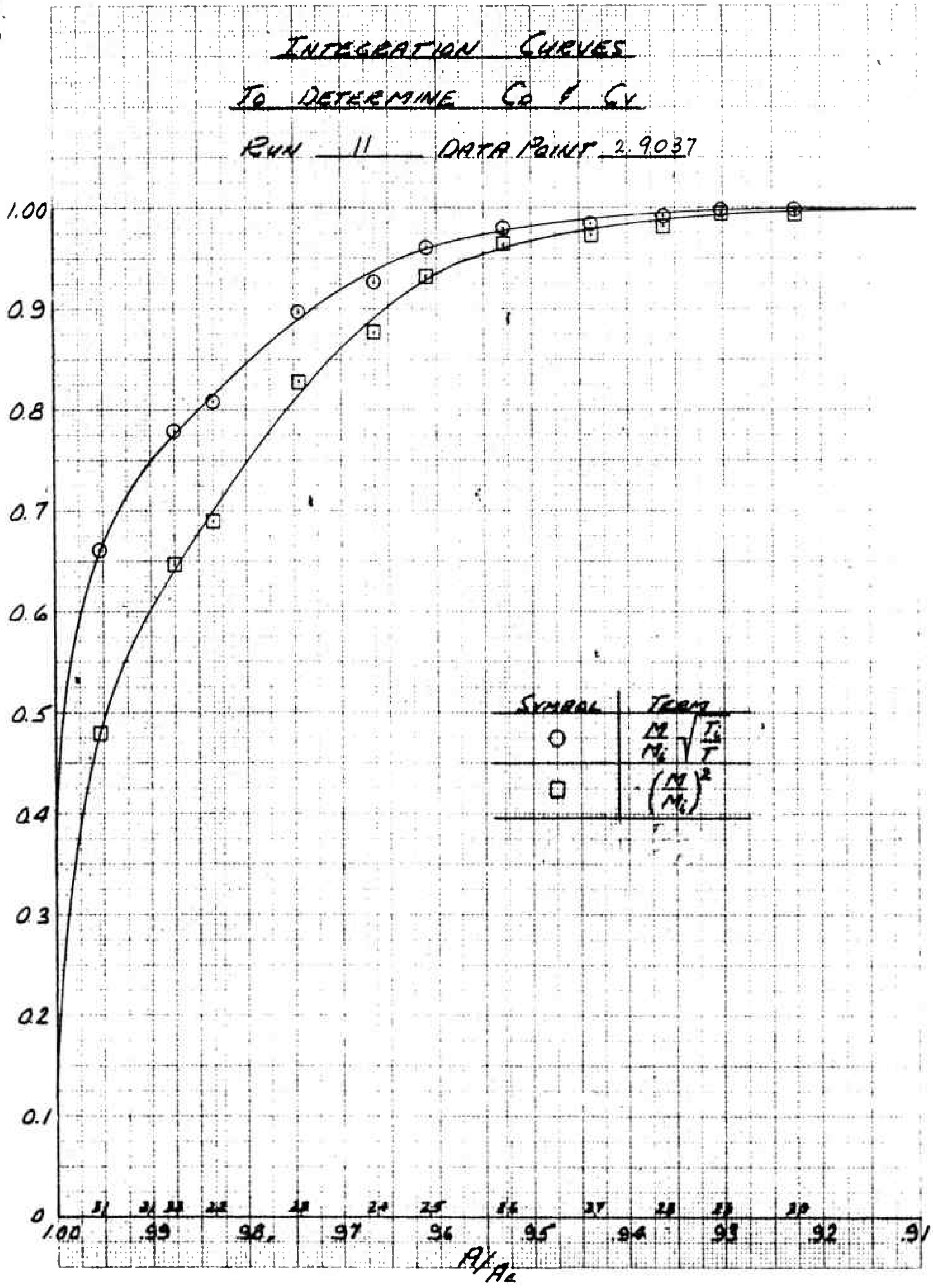
INTEGRATION CURVES
TO DETERMINE C_D & C_V
RUN 11 DATA POINT 2.9037
1.00
0.9
0.8
0.7
0.6
0.5
0.4
0.3
0.2
0.1
0
SYMBAL
TERM
$\frac{M}{M_i}\sqrt{\frac{T_i}{T}}$
$\left(\frac{M}{M_i}\right)^2$
1.00
.99
.98
.97
.96
.95
.94
.93
.92
.91
A_x/A_e

FLUIDYNE ENGINEERING CORPORATION

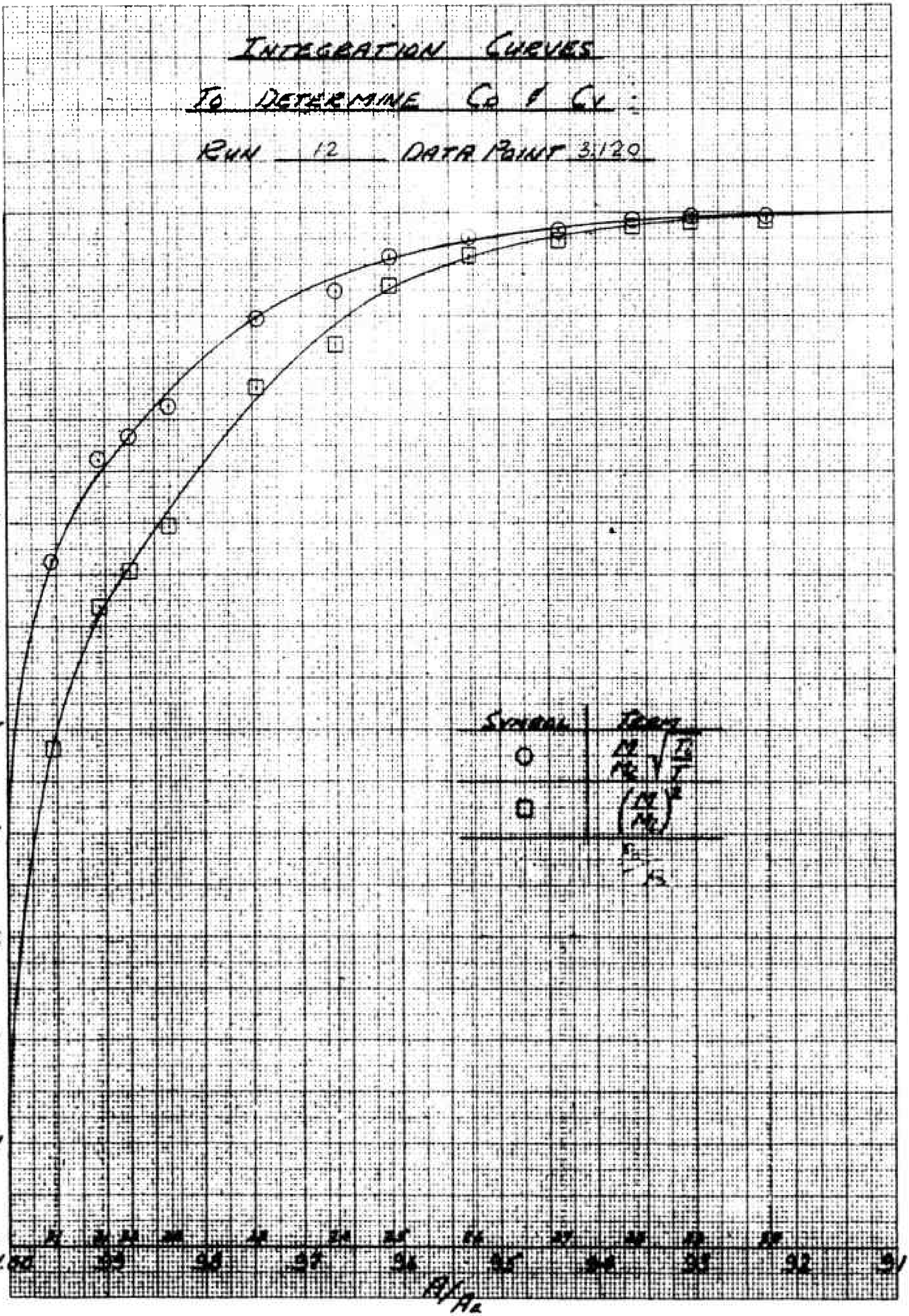

3386
5266

FLUIDYNE ENGINEERING CORPORATION

INTEGRATION CURVES
TO DETERMINE C_D & C_V

RUN 13 DATA POINT 3.355

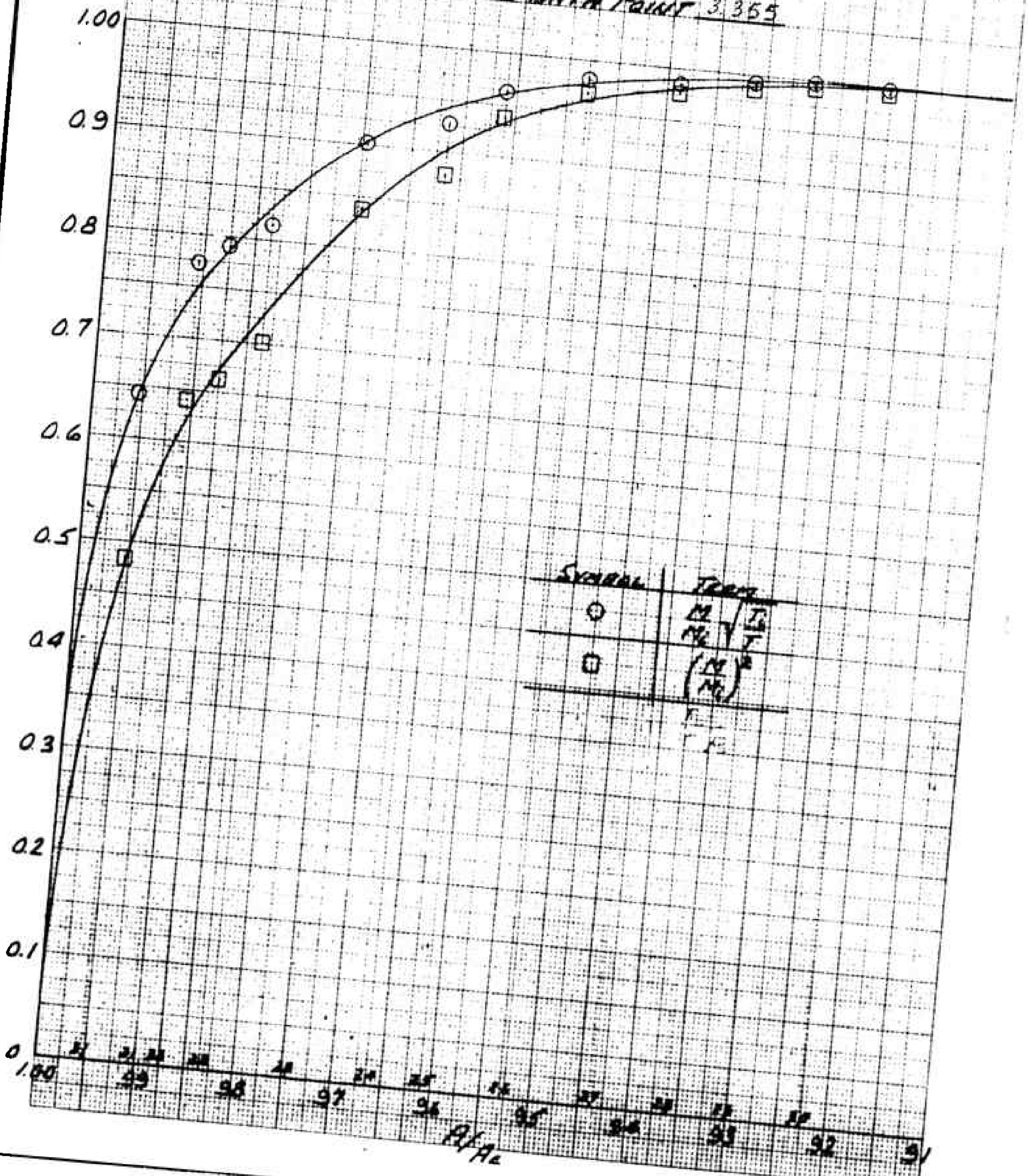

FluiDyne ENGINEERING CORPORATION

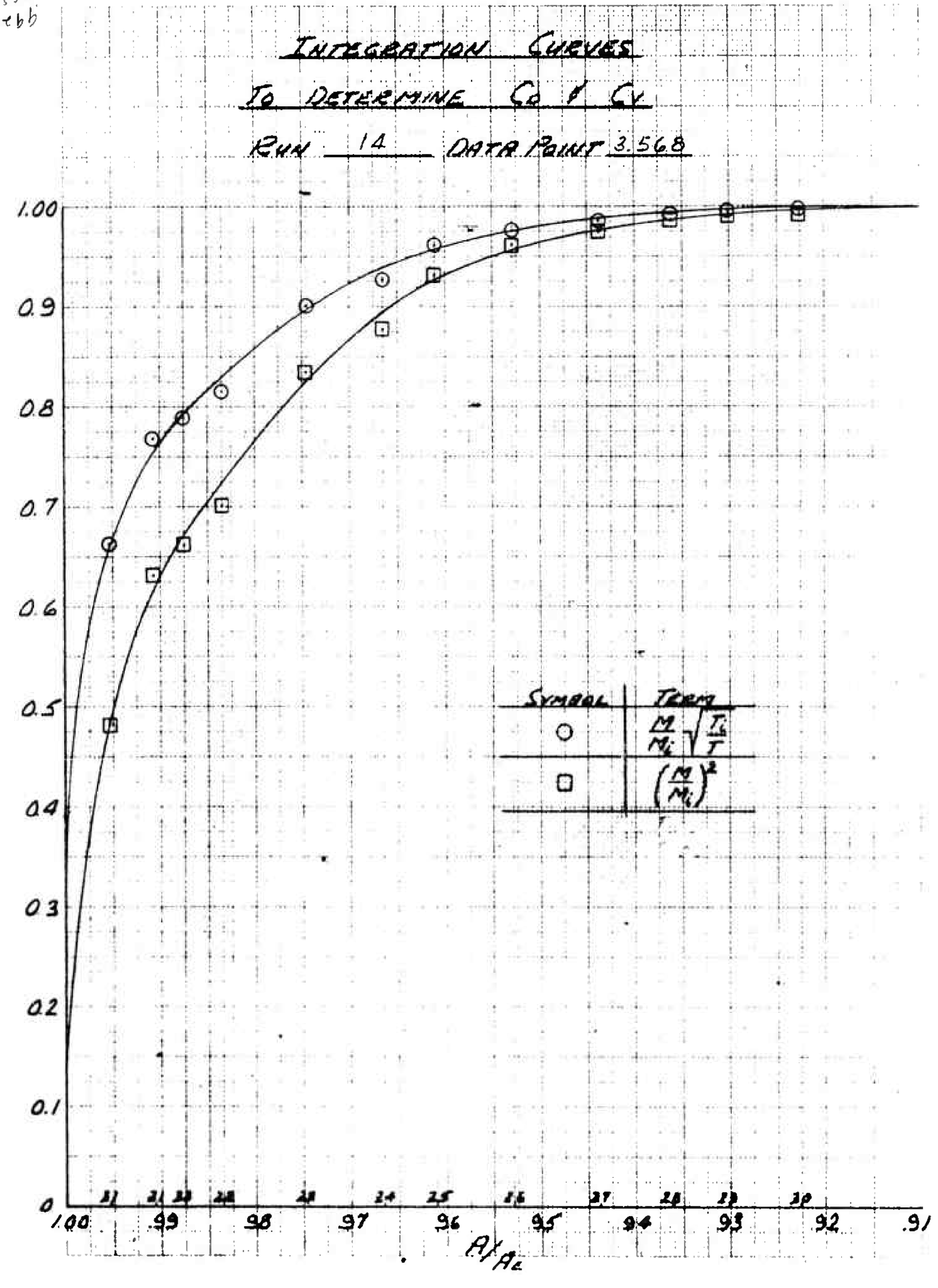

FluiDyne Engineering Corporation

INTEGRATION CURVES
TO DETERMINE C_D & C_V
RUN 15 DATA POINT 3.773

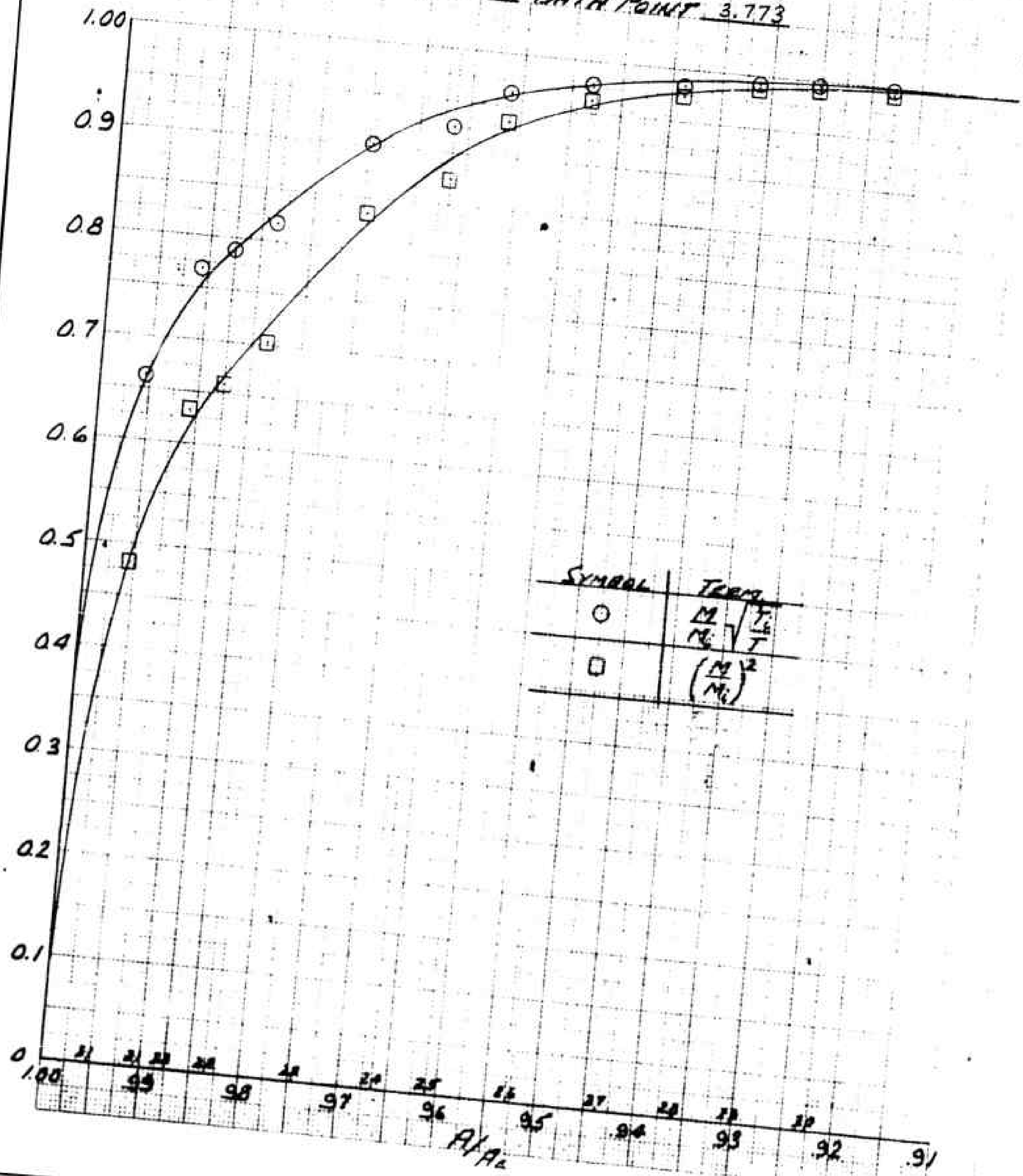

INTEGRATION CURVES

TO DETERMINE C_D & C_V

RUN 16 a DATA POINT 3.985

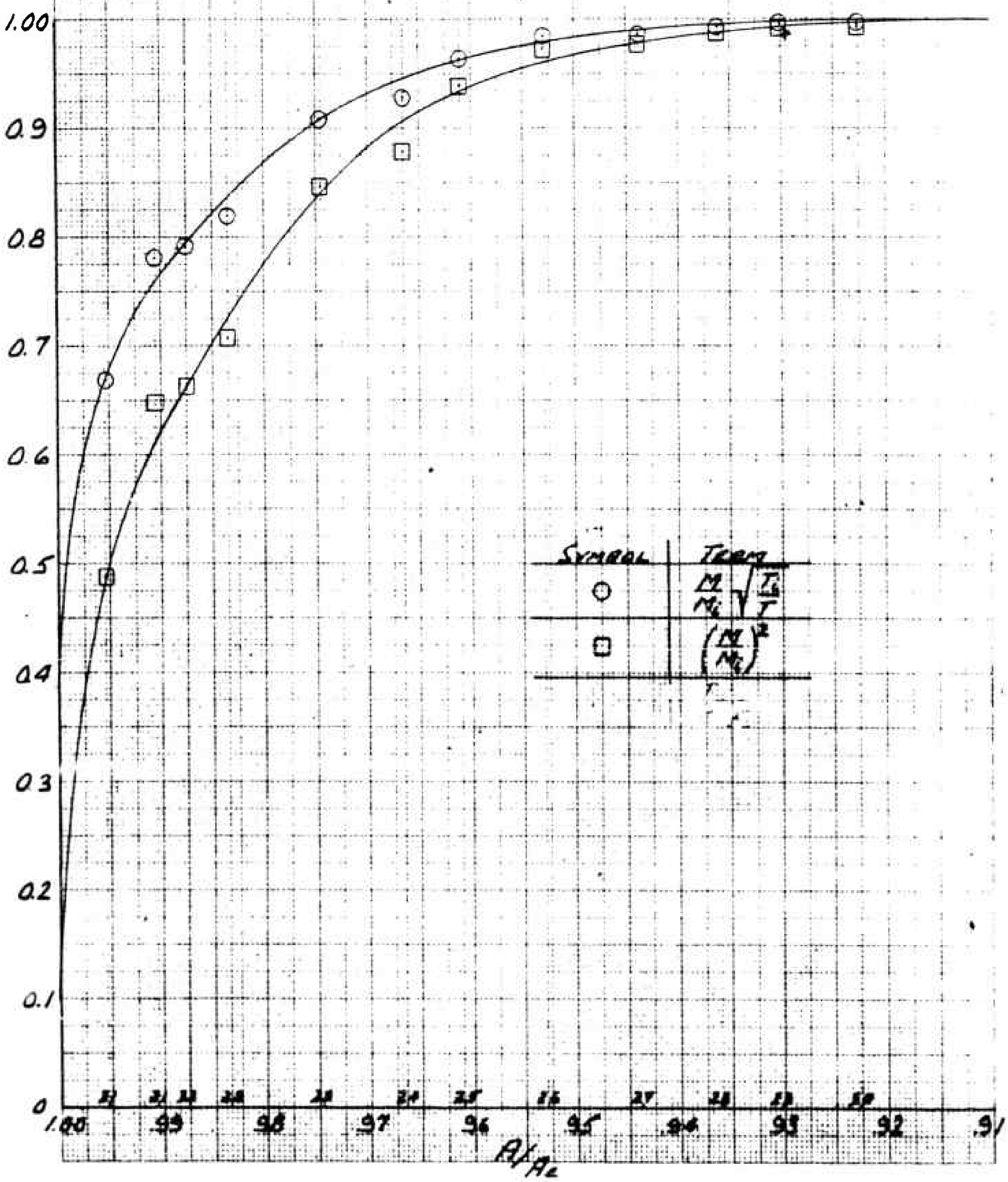

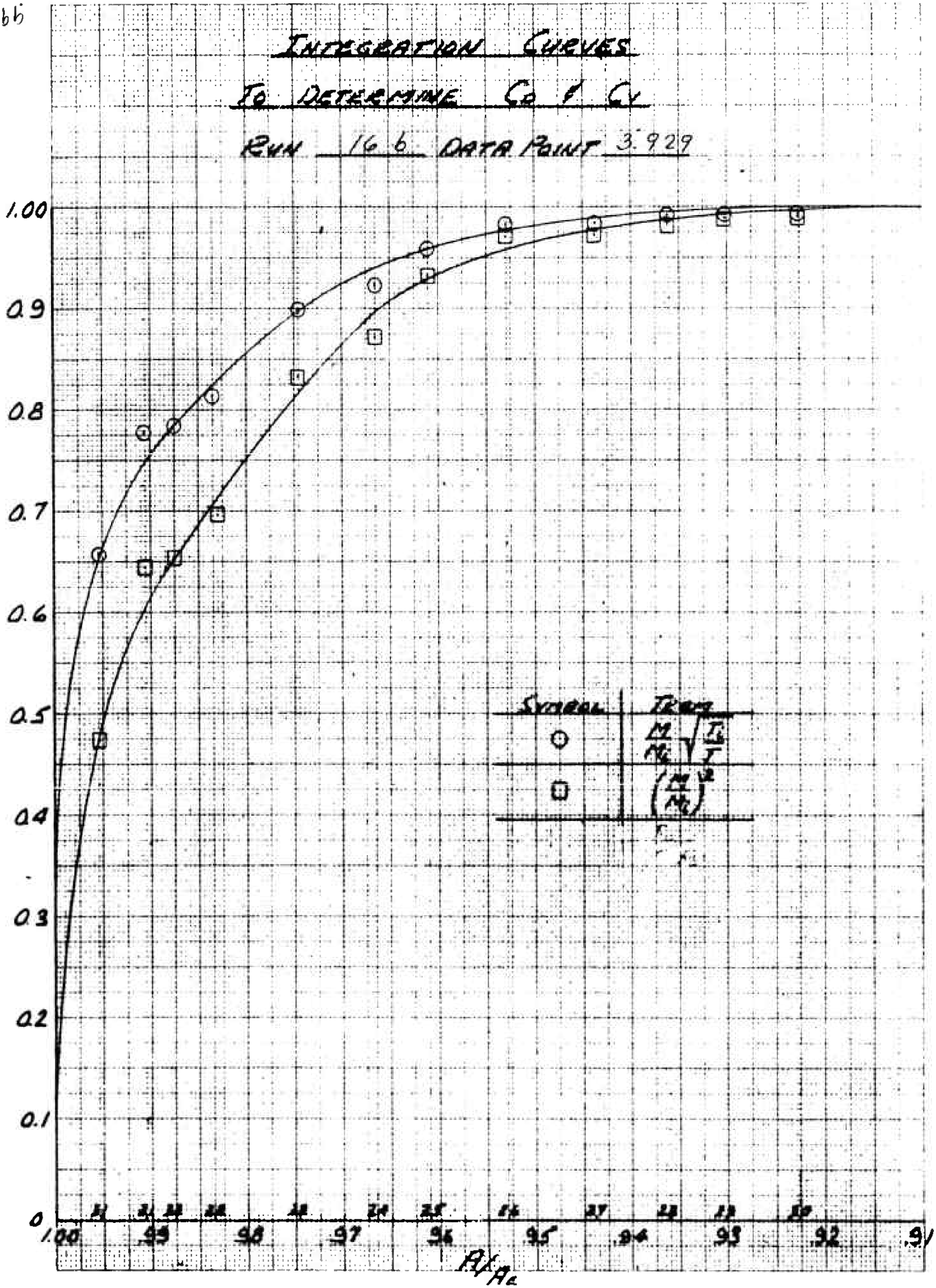
INTEGRATION CURVES
TO DETERMINE C_D & C_V
RUN 16 b DATA POINT 3.929
1.00
0.9
0.8
0.7
0.6
0.5
0.4
0.3
0.2
0.1
0
1.00
.99
.98
.97
.96
.95
.94
.93
.92
.91
A/Ae
SYMBOL
TERM
$\frac{M}{M_c}\sqrt{\frac{T_c}{T}}$
$\left(\frac{M}{M_c}\right)^2$

FLUIDYNE ENGINEERING CORPORATION

INTEGRATION CURVES

TO DETERMINE C_D & C_V

RUN 17 DATA POINT 1.2192

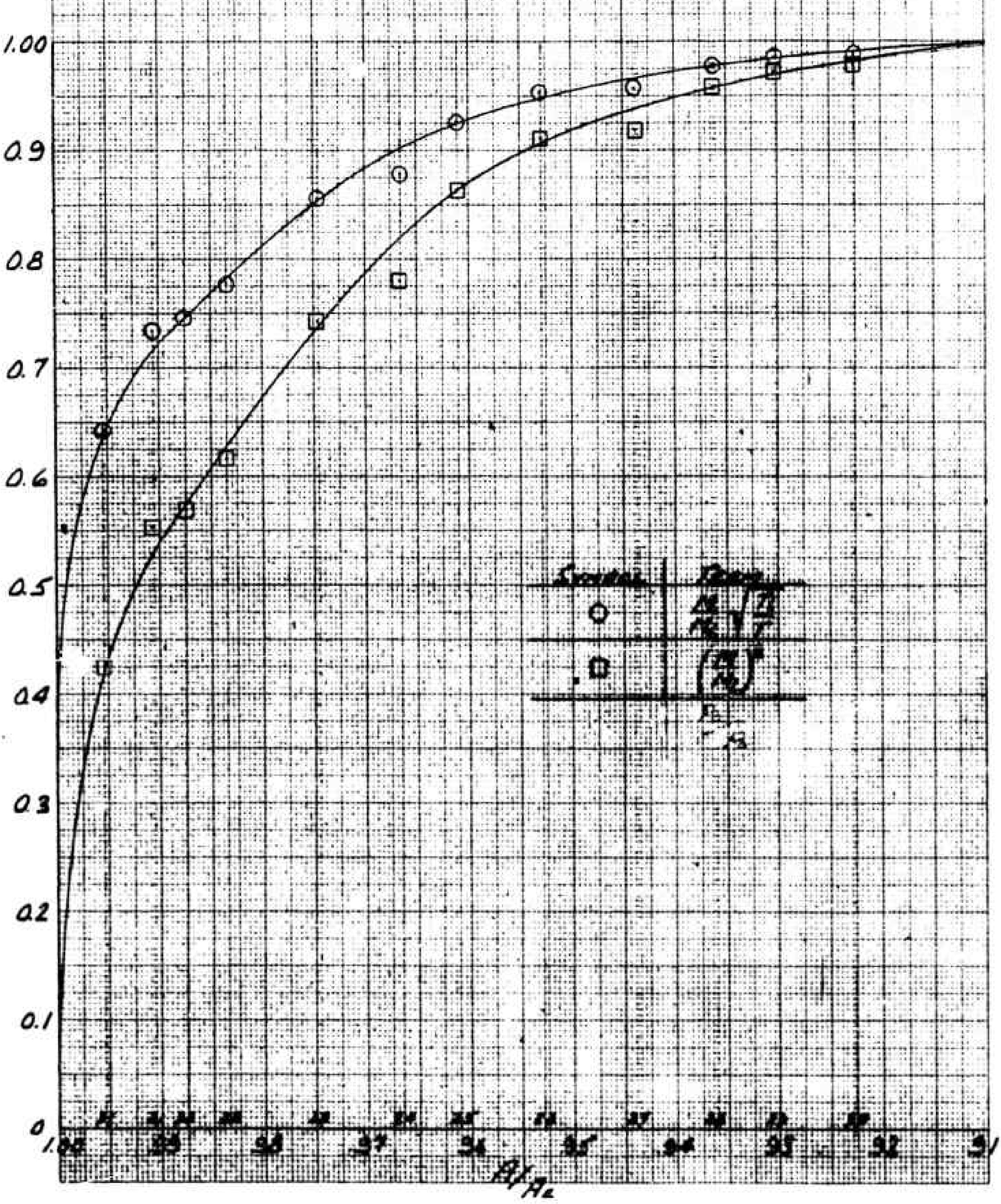

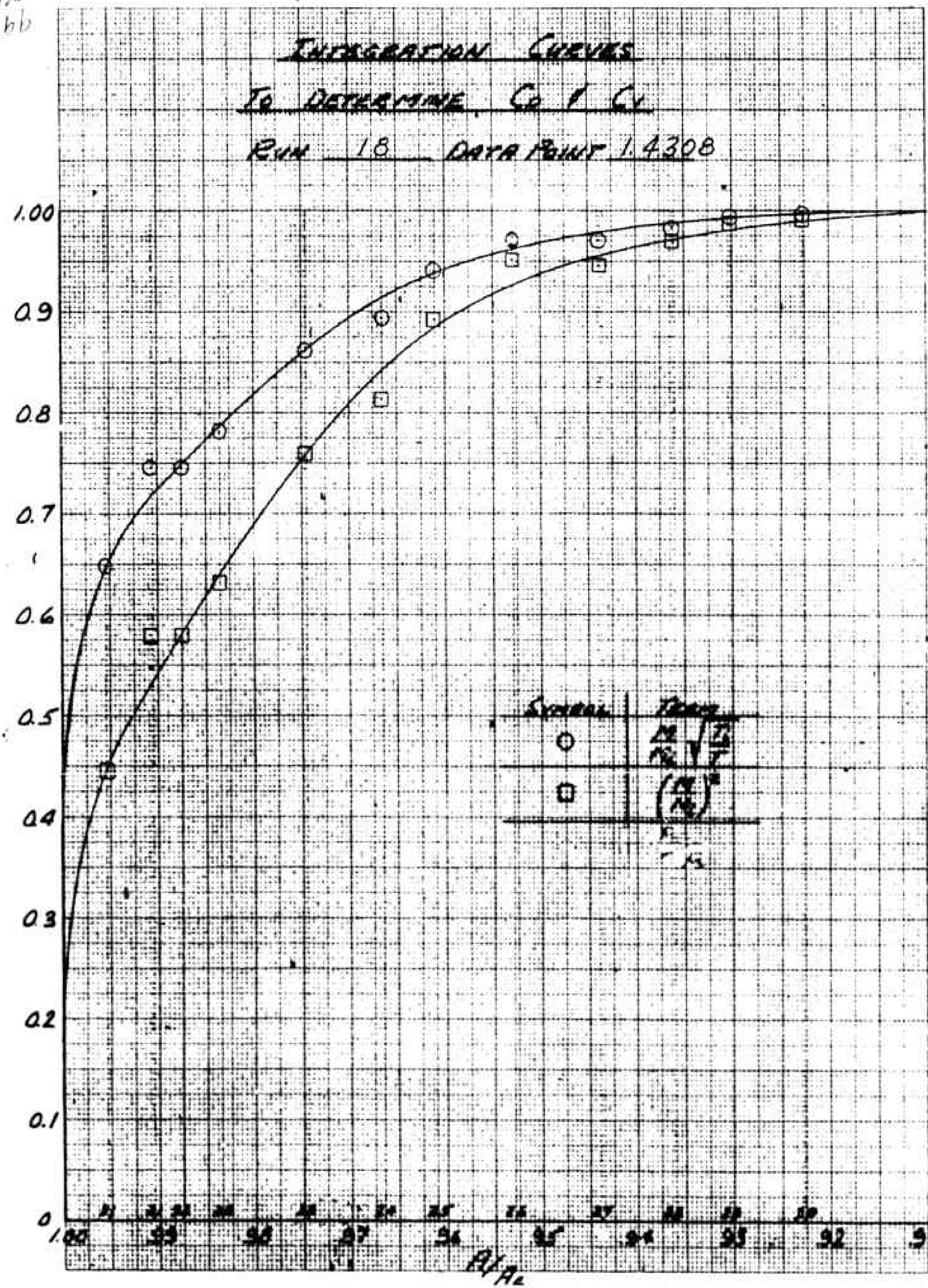
INTEGRATION CURVES
TO DETERMINE C_D & C_V
RUN 18 DATA POINT 1.4308
1.00
0.9
0.8
0.7
0.6
0.5
0.4
0.3
0.2
0.1
0
1.00
.99
.98
.97
.96
.95
.94
.93
.92
.91
A/A_c
SYMBOL
TERM

FLUIDYNE ENGINEERING CORPORATION

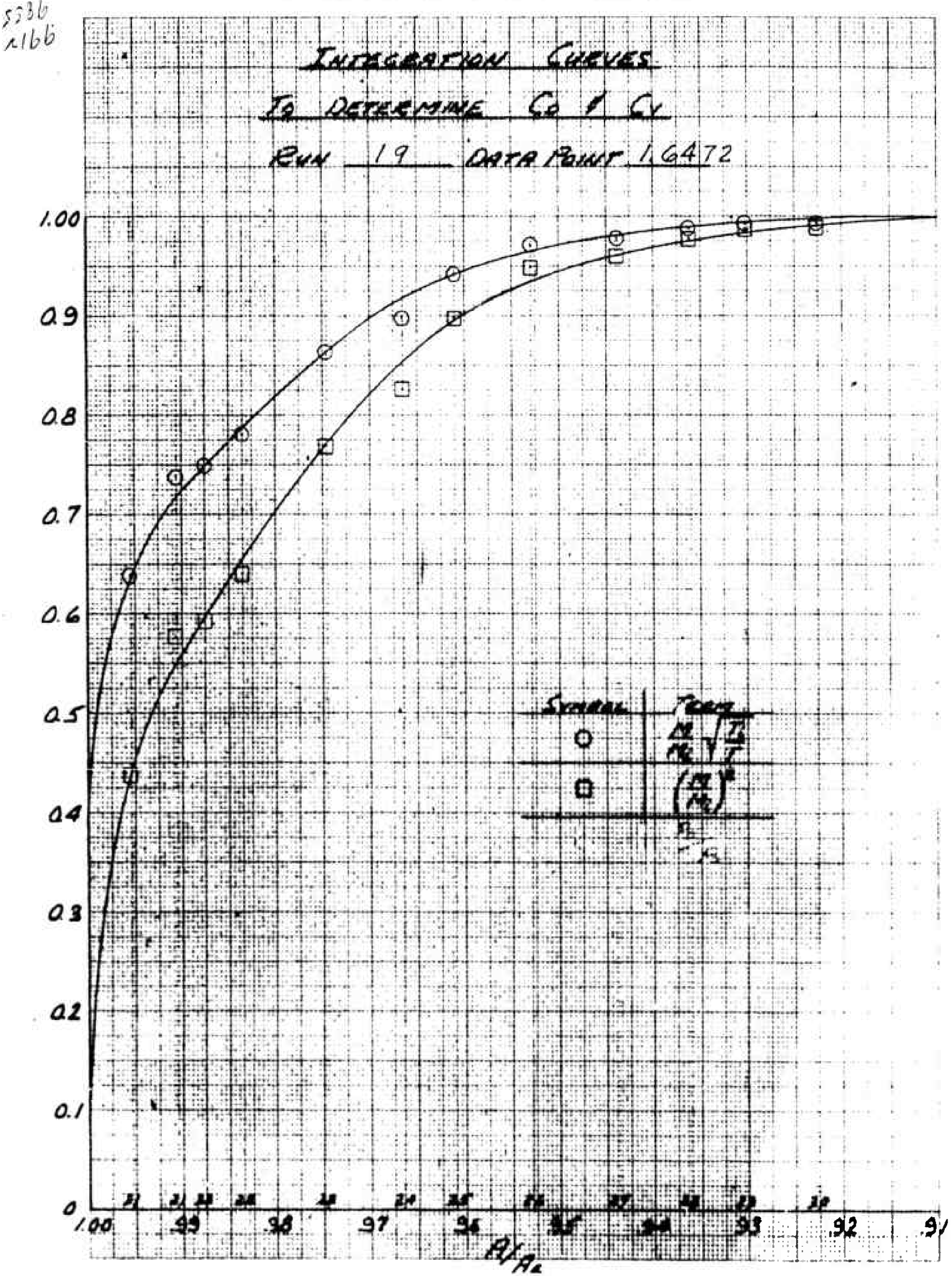

FluiDyne Engineering Corporation

Integration Curves To Determine Cd & Cv

Run 20 Data Point 1.6133

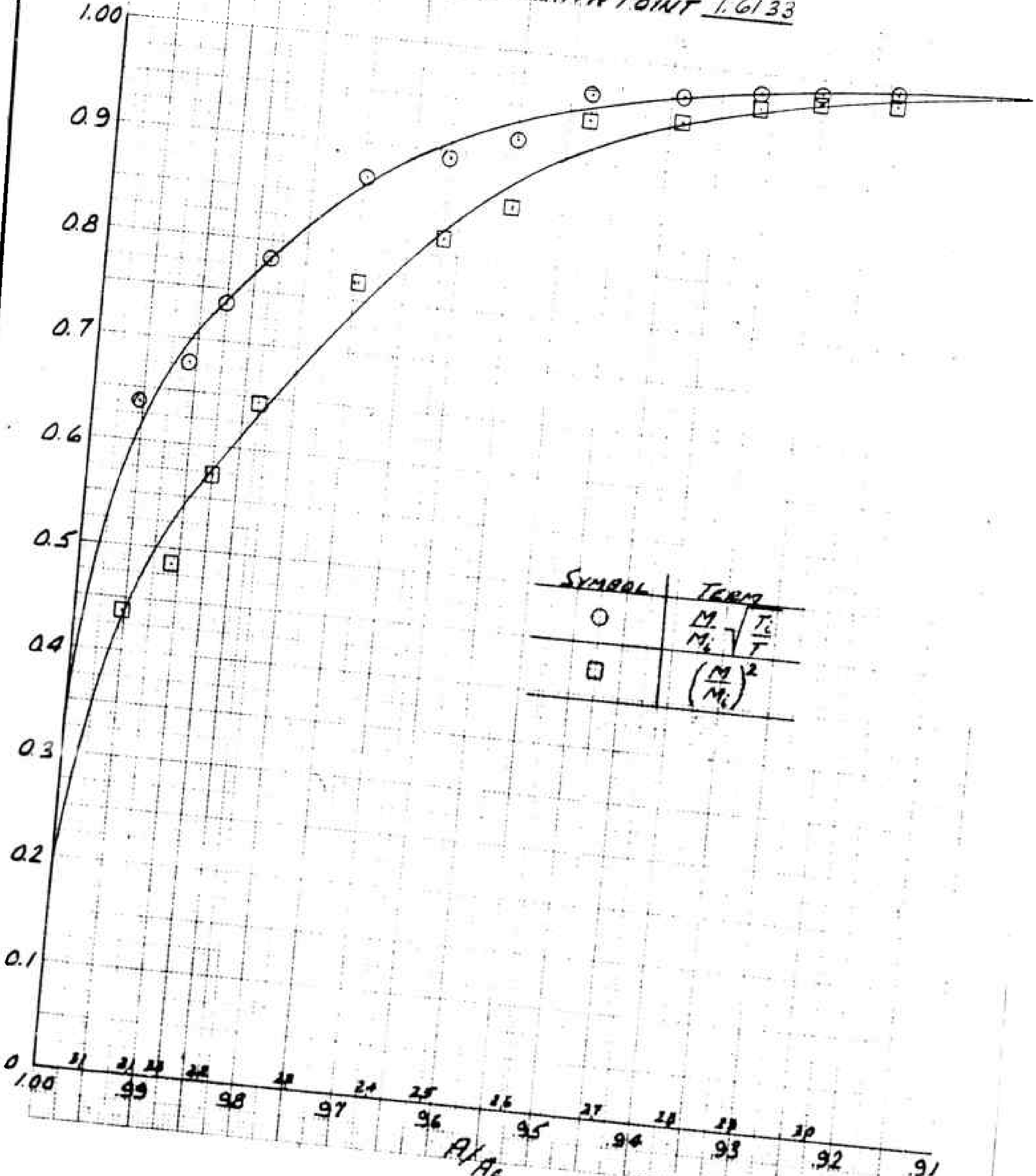

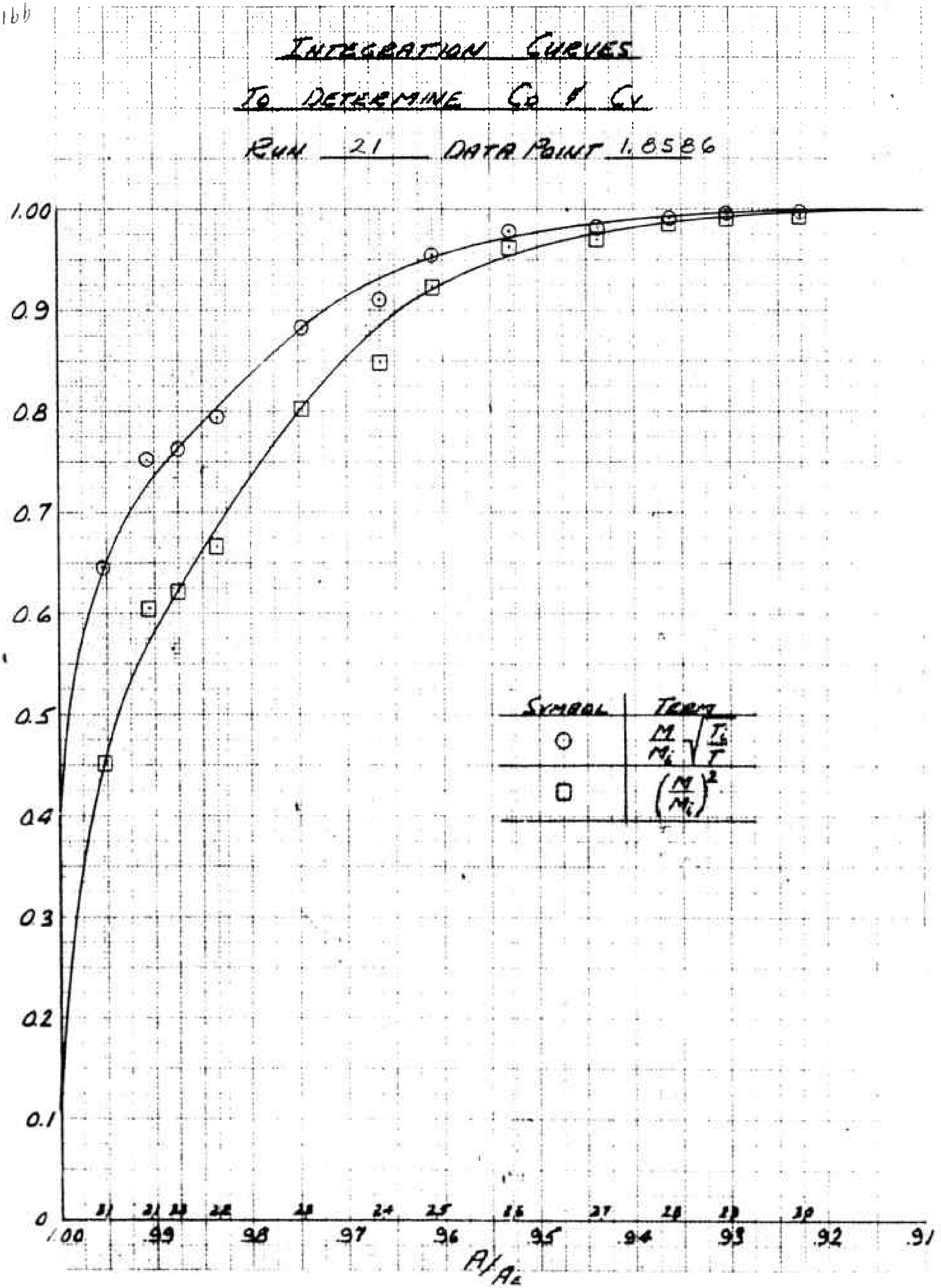
INTEGRATION CURVES
TO DETERMINE C_D & C_V
RUN 21 DATA POINT 1.8586
SYMBOL
TERM
$\frac{M}{M_i}\sqrt{\frac{T_i}{T}}$
$\left(\frac{M}{M_i}\right)^2$
1.00
0.9
0.8
0.7
0.6
0.5
0.4
0.3
0.2
0.1
0
1.00
.99
.98
.97
.96
.95
.94
.93
.92
.91
A/A_i

FLUIDYNE ENGINEERING CORPORATION

INTEGRATION CURVES
TO DETERMINE C_D & C_V

RUN 22 DATA POINT 2.066

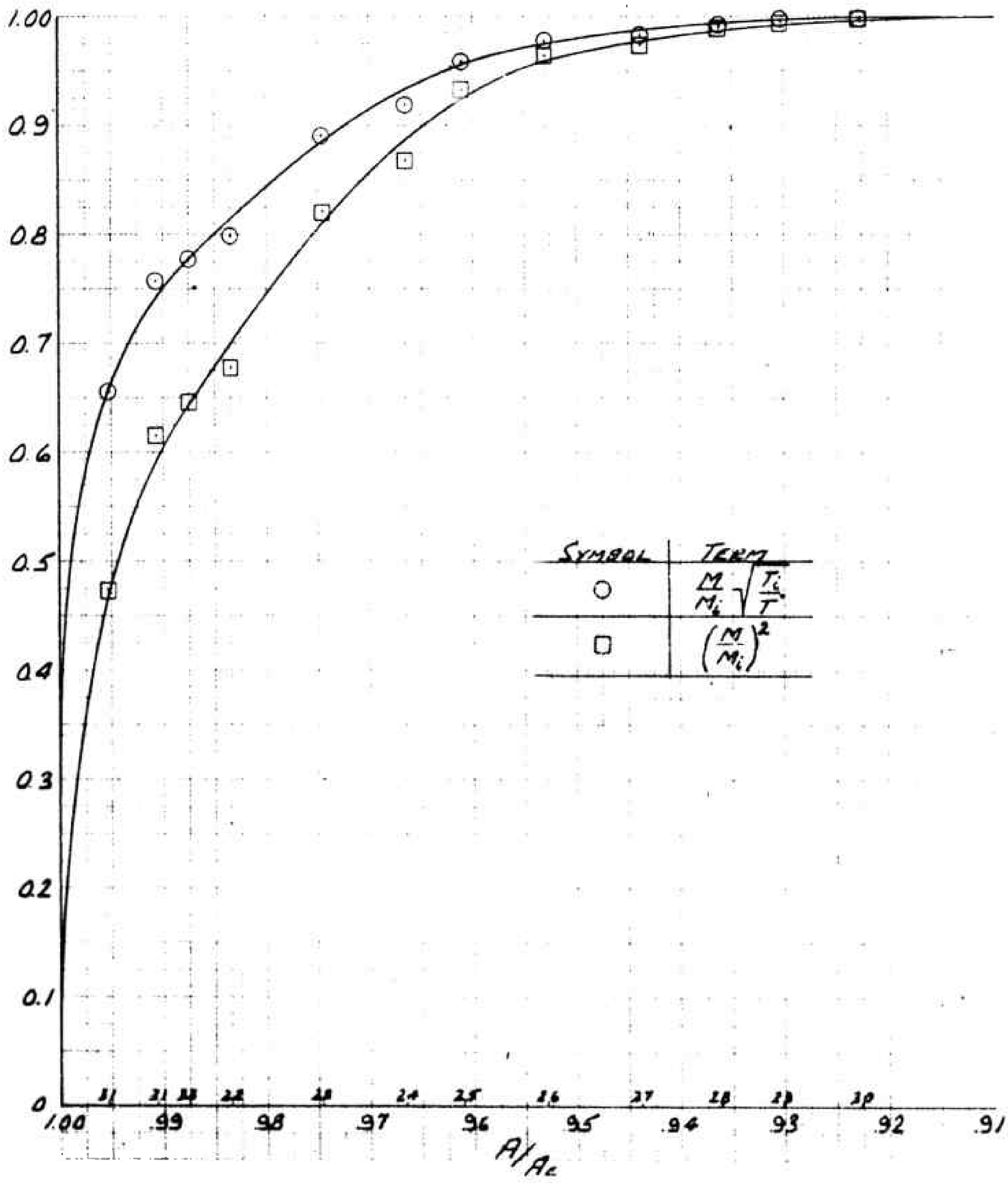

FLUIDYNE ENGINEERING CORPORATION

9923
9876

INTEGRATION CURVES
TO DETERMINE C_D & C_V
RUN 23 DATA POINT 2.0734

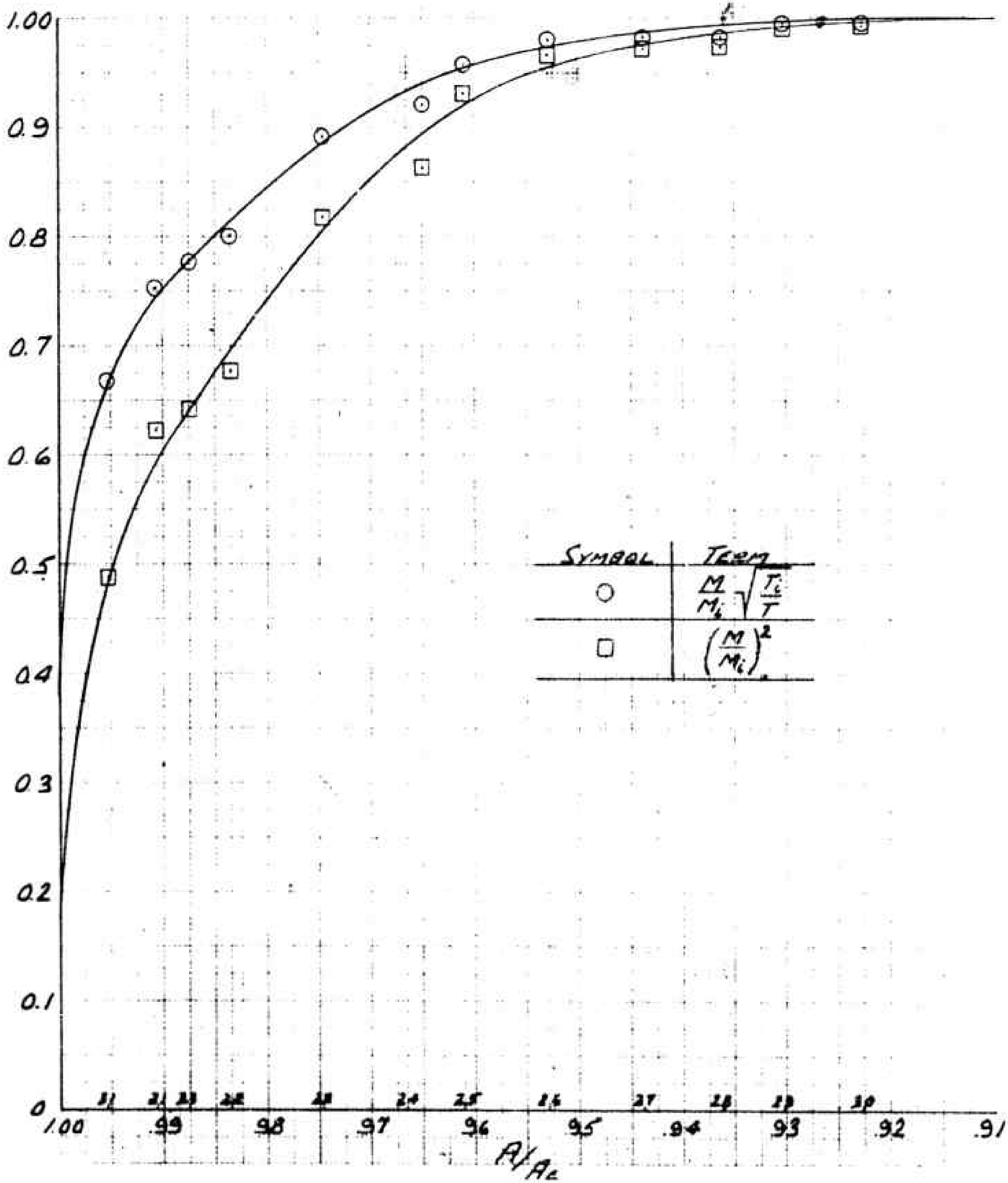

FLUIDYNE ENGINEERING CORPORATION

9843
9908

INTEGRATION CURVES

TO DETERMINE C_D & C_V

RUN 24 DATA POINT 1.2133

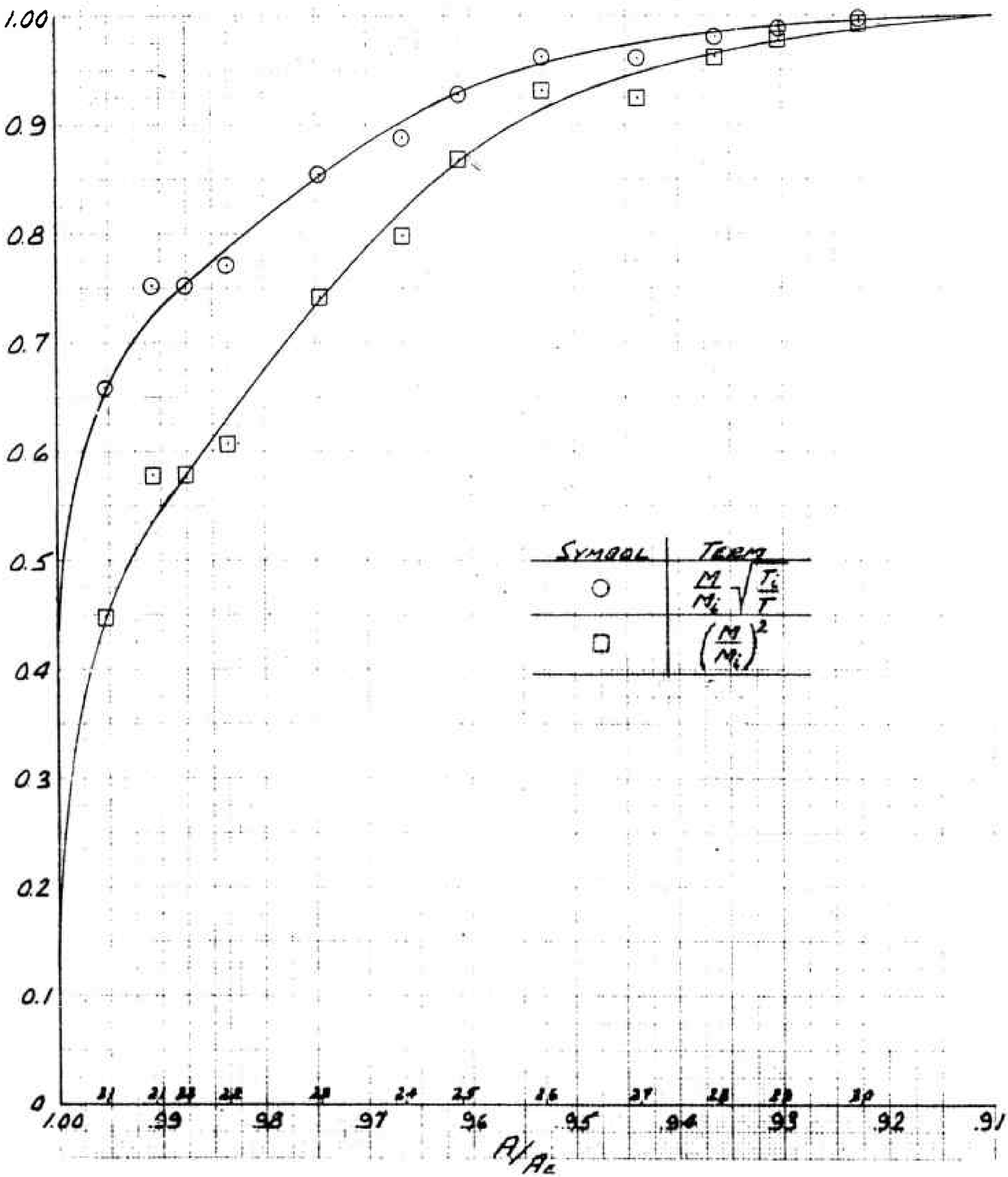

FLUIDYNE ENGINEERING CORPORATION

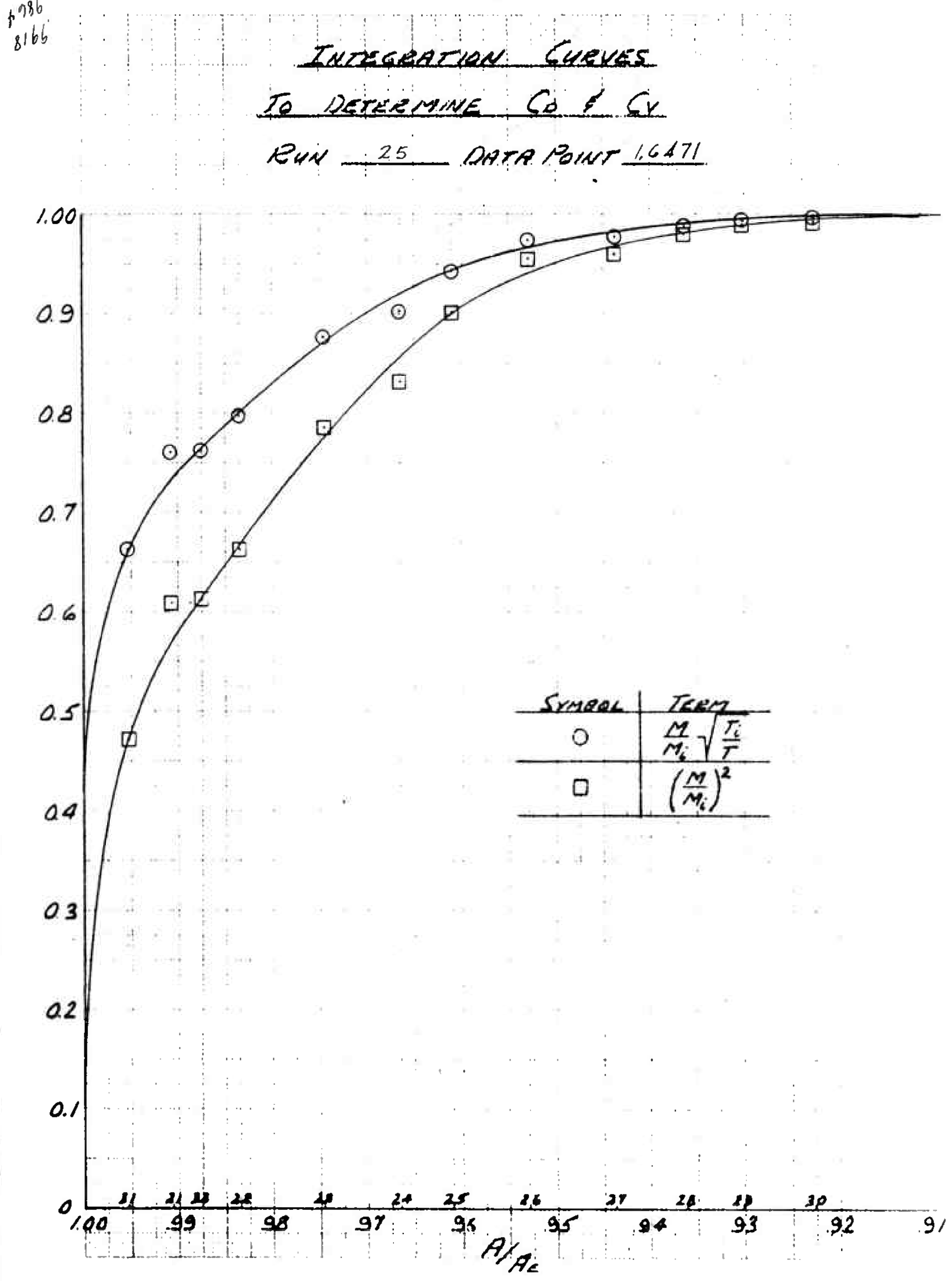

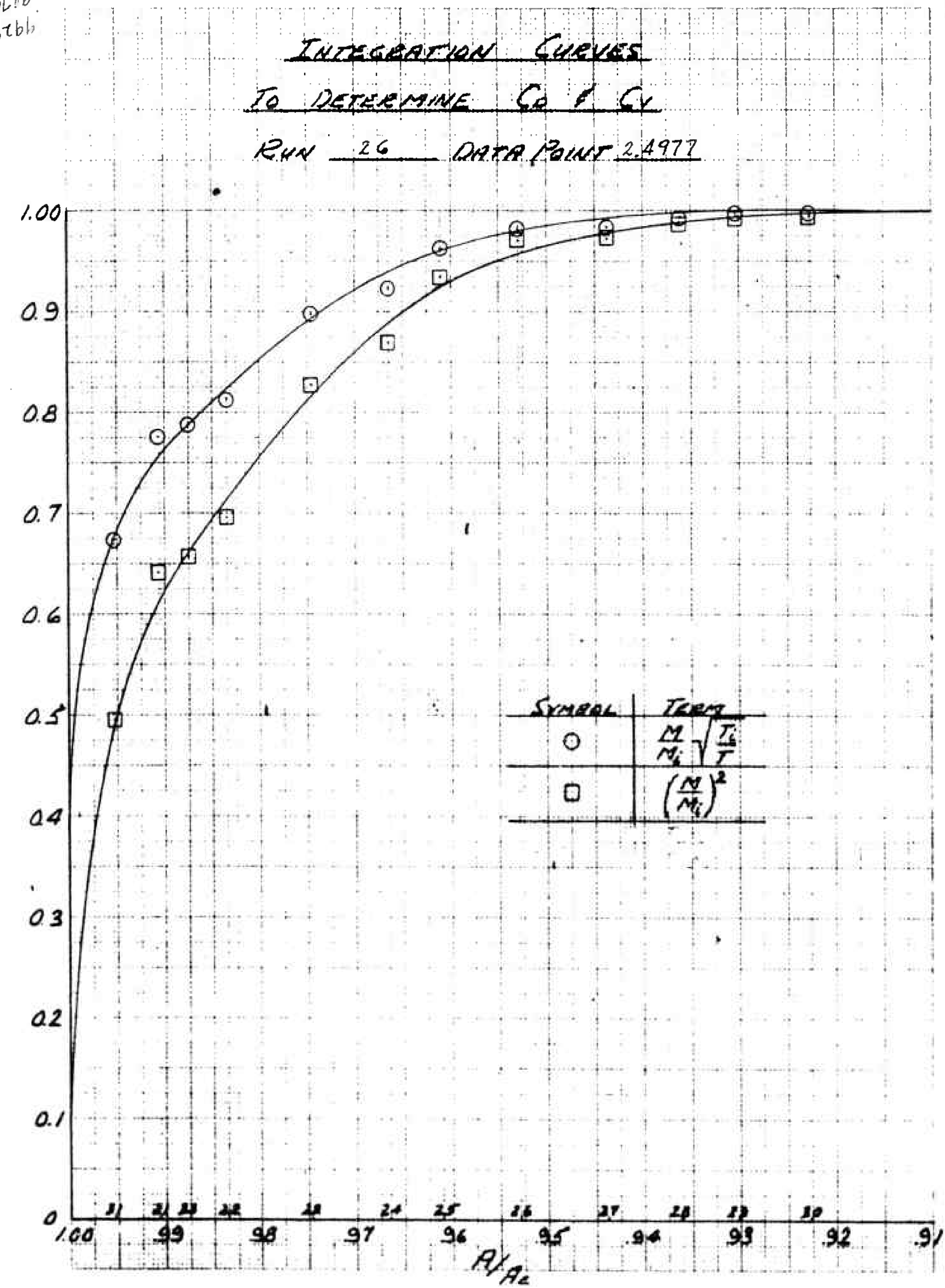
INTEGRATION CURVES
TO DETERMINE C_D & C_V
RUN 26 DATA POINT 2.4977
1.00
0.9
0.8
0.7
0.6
0.5
0.4
0.3
0.2
0.1
0
1.00
.99
.98
.97
.96
.95
.94
.93
.92
.91
A/A_L
SYMBOL
TERM
$\frac{M}{M_i}\sqrt{\frac{T_i}{T}}$
$\left(\frac{M}{M_i}\right)^2$

INTEGRATION CURVES TO DETERMINE C_D & C_V

RUN 27 DATA POINT 2.4884

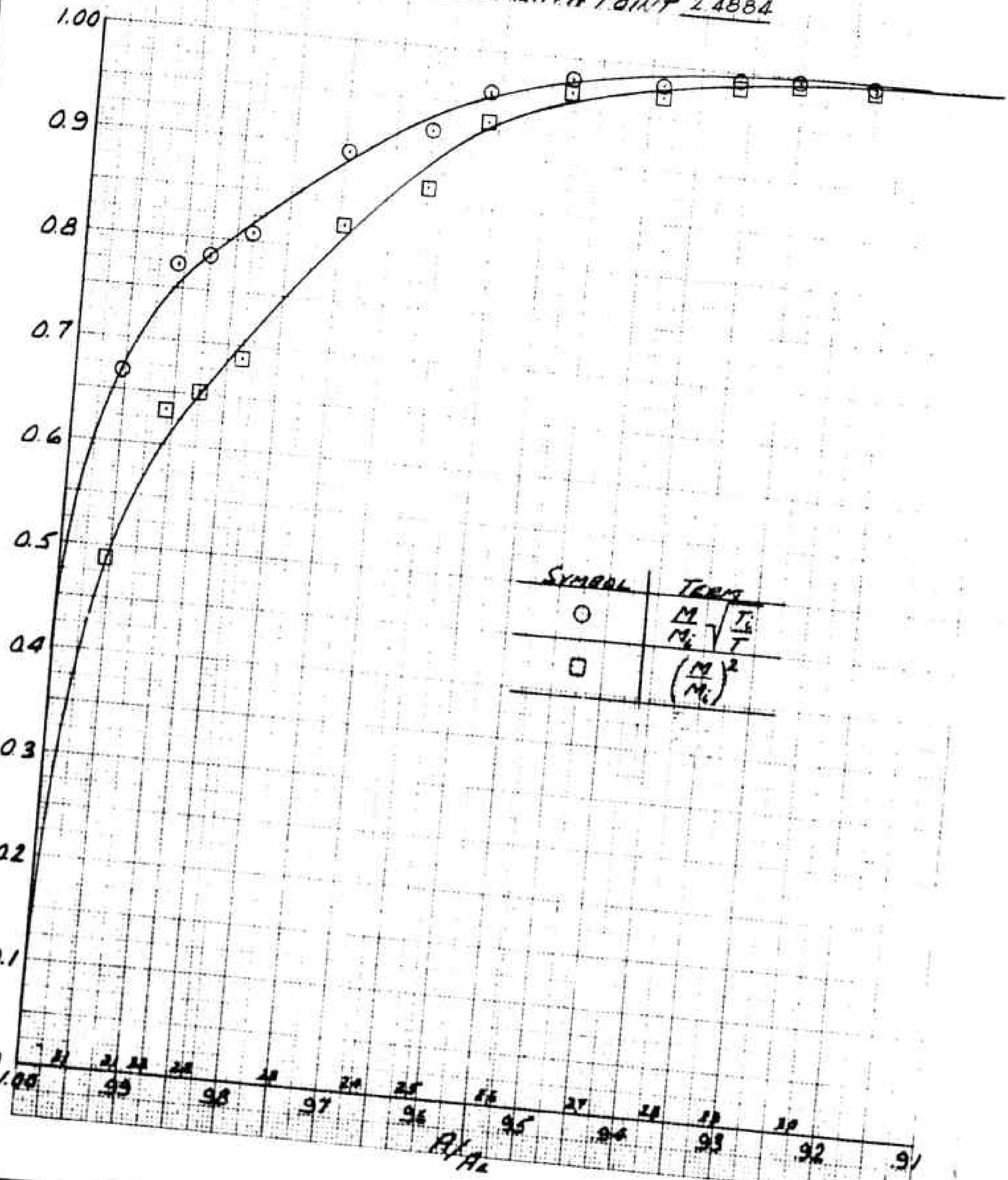

FLUIDYNE ENGINEERING CORPORATION

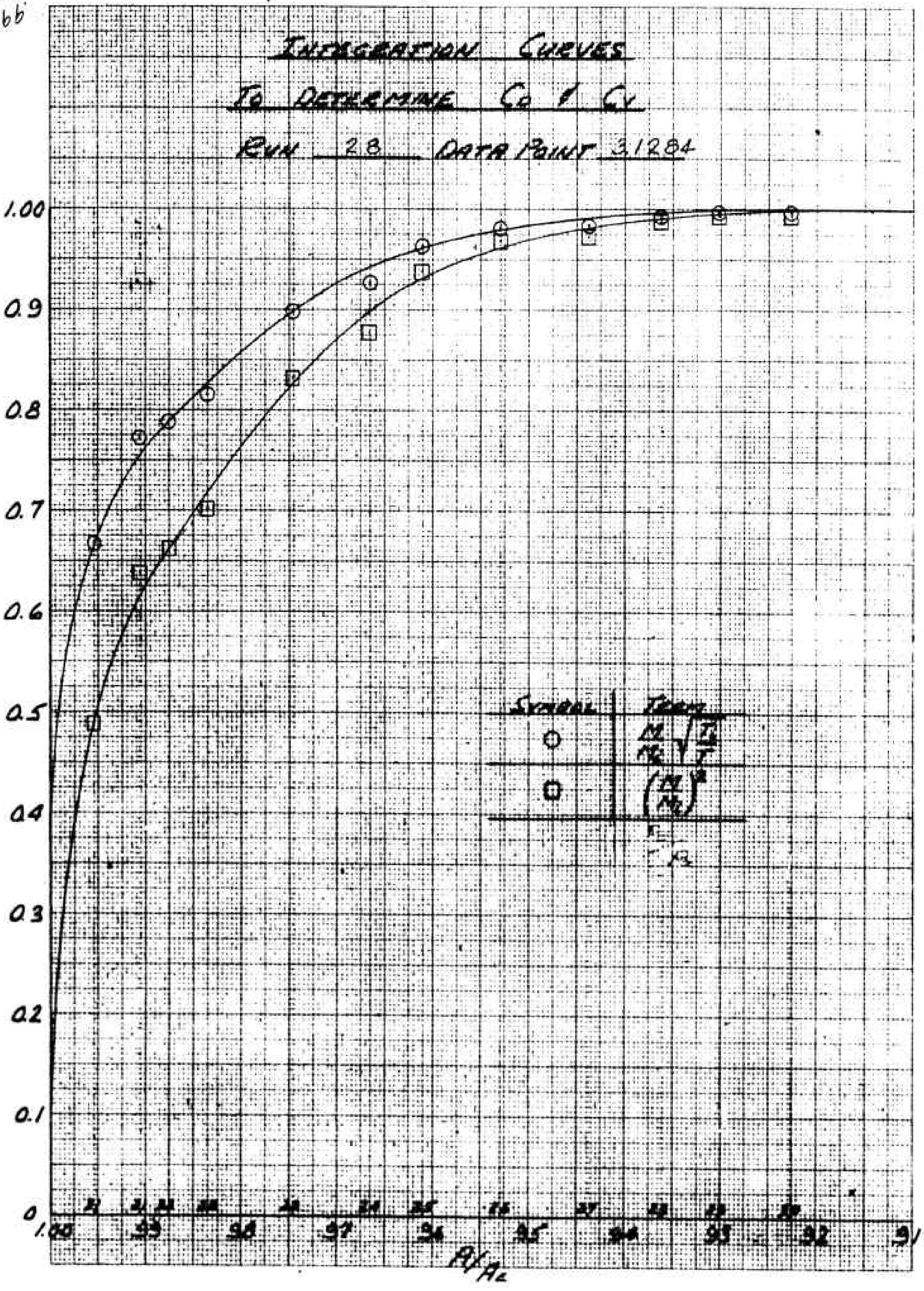

FLUIDYNE ENGINEERING CORPORATION

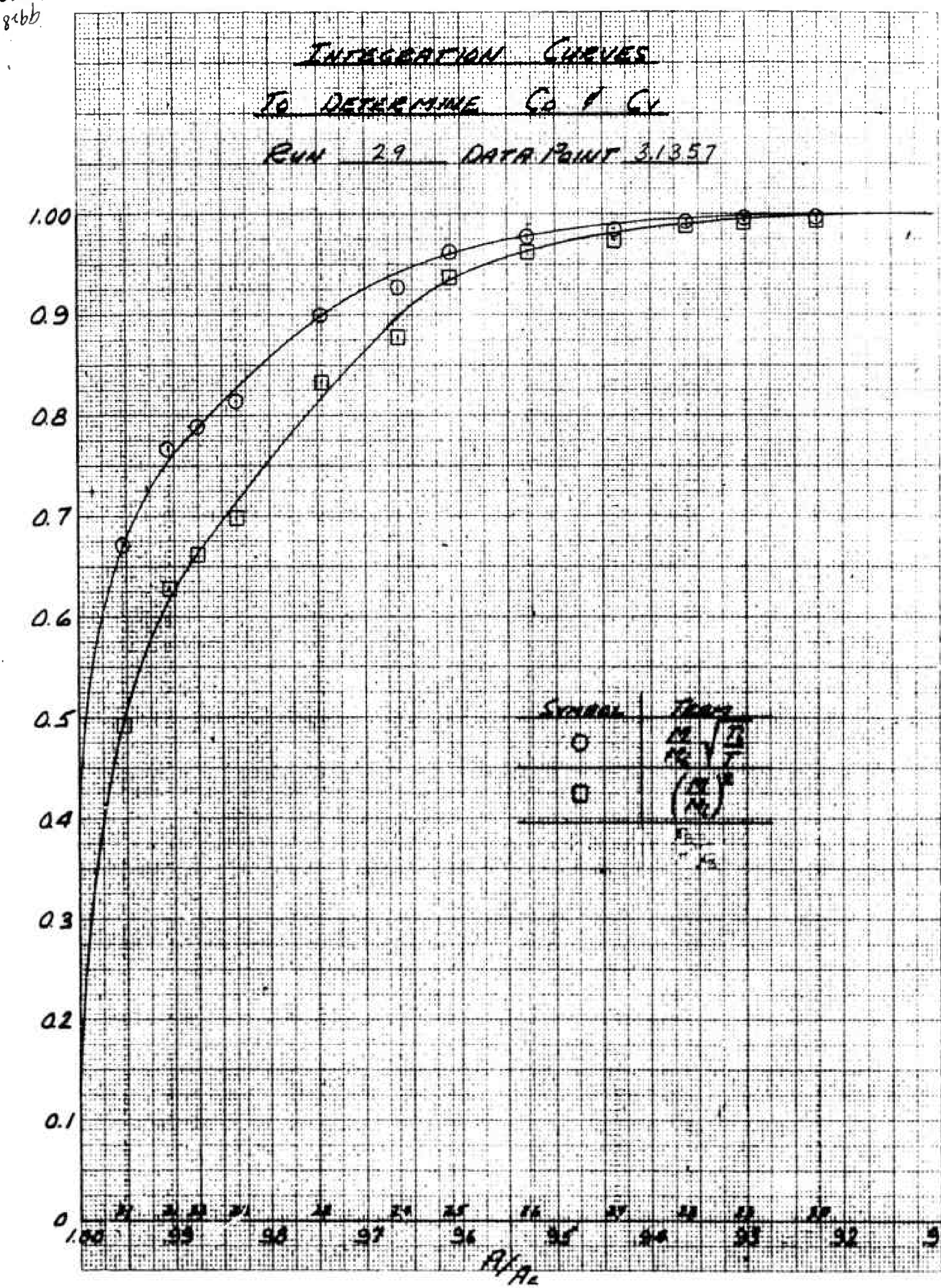

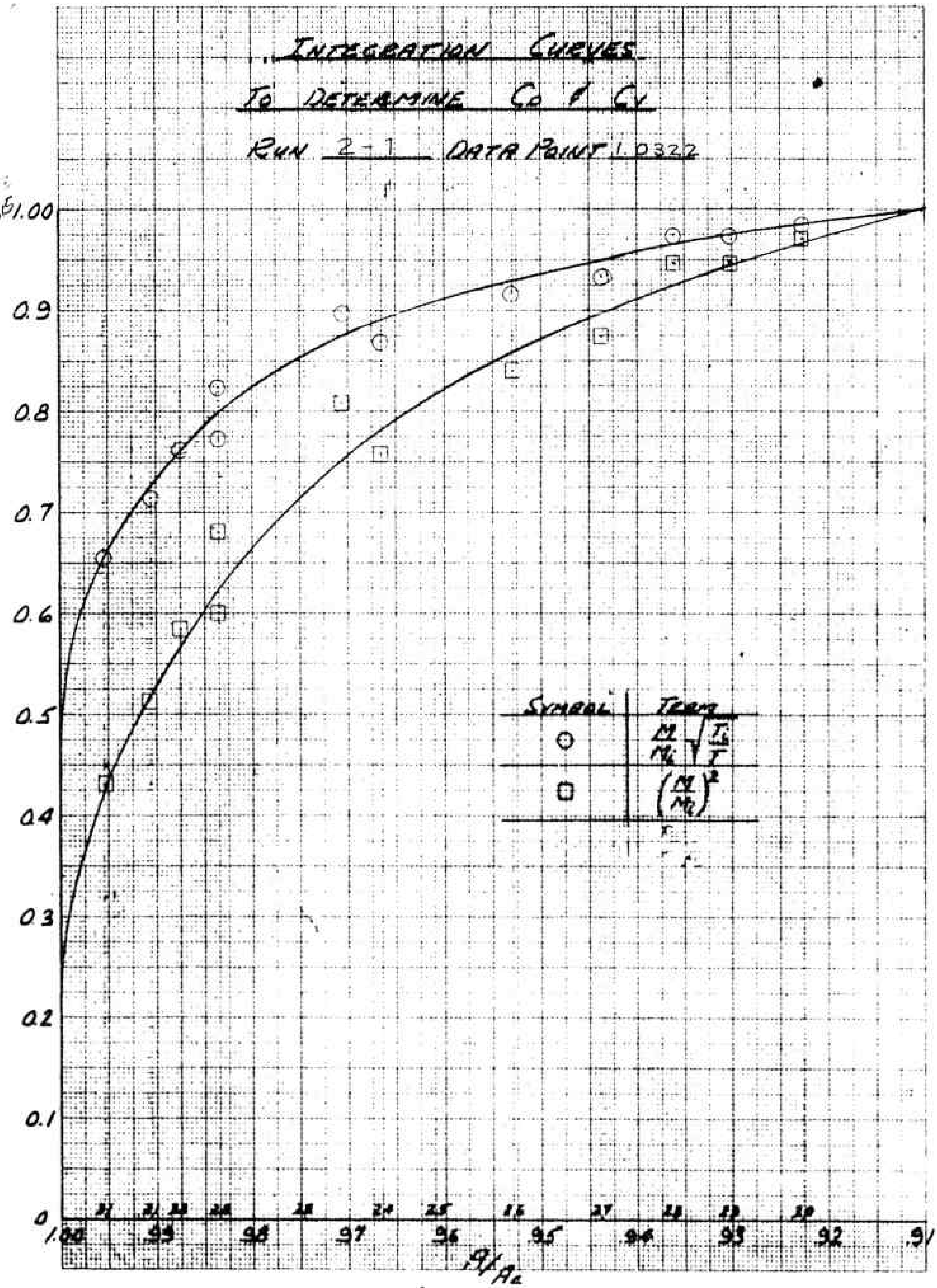
INTEGRATION CURVES
TO DETERMINE Cd & Cv
RUN 2-1 DATA POINT 1.0322
1.00
0.9
0.8
0.7
0.6
0.5
0.4
0.3
0.2
0.1
0
1.00
.99
.98
.97
.96
.95
.94
.93
.92
.91
SYMBOL
TERM
$\frac{M}{M_i}\sqrt{\frac{T_i}{T}}$
$\left(\frac{M}{M_i}\right)^2$
A/A_c

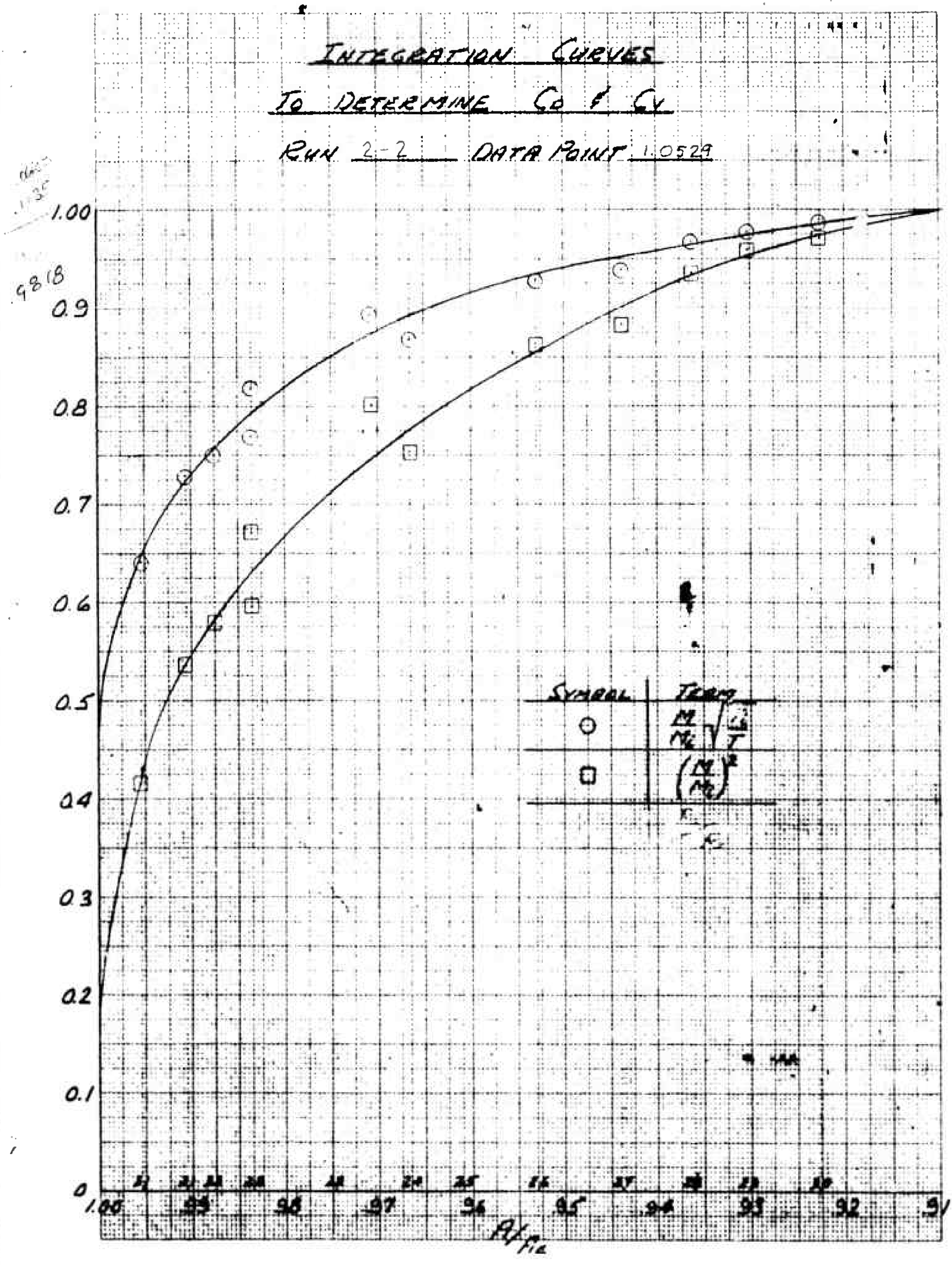
INTEGRATION CURVES
TO DETERMINE Cd & Cv
RUN 2-2 DATA POINT 1.0529
1.00
0.9
0.8
0.7
0.6
0.5
0.4
0.3
0.2
0.1
0
1.00
.99
.98
.97
.96
.95
.94
.93
.92
.91
SYMBOL
TERM
P/P_c

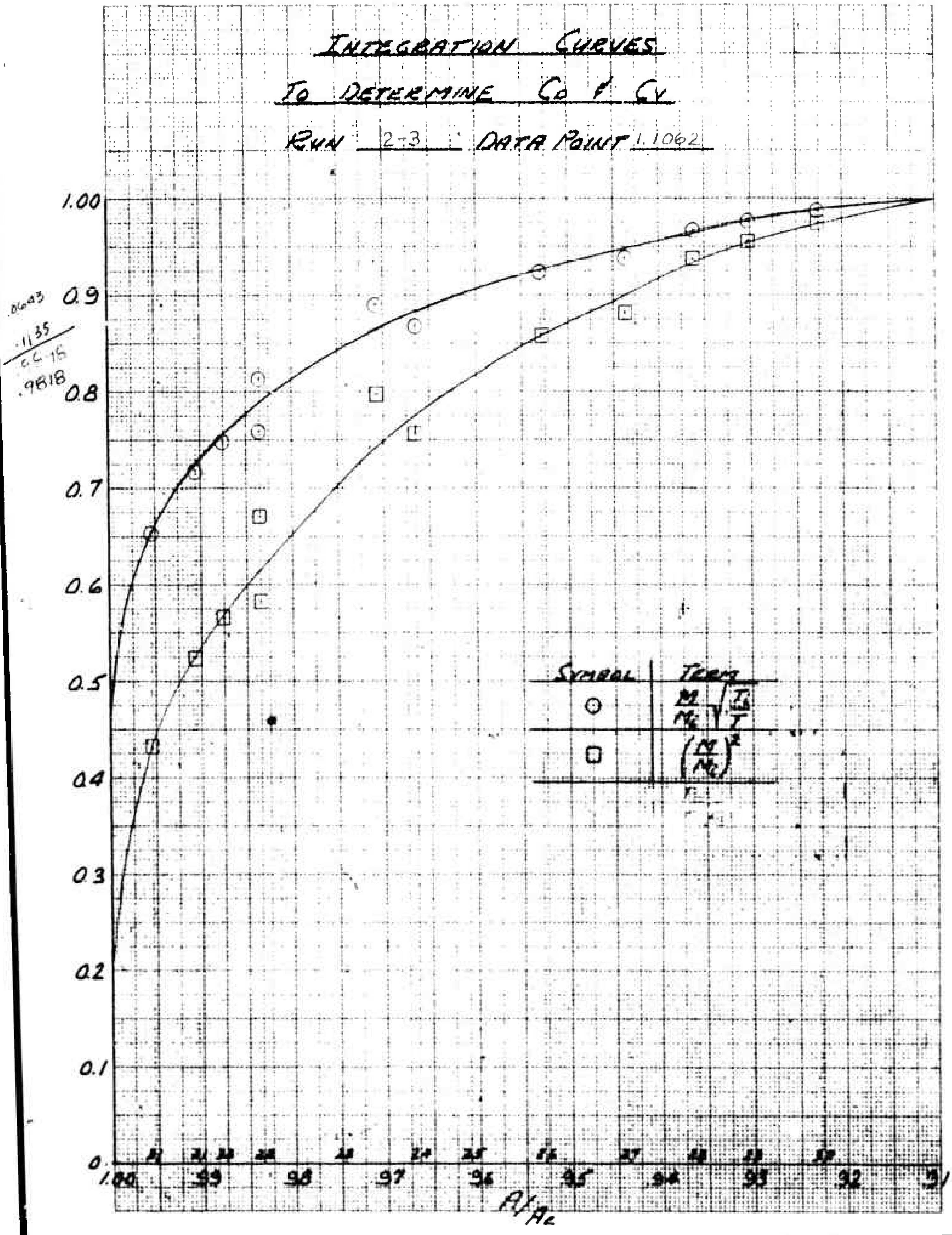
INTEGRATION CURVES
TO DETERMINE C_D & C_V
RUN 2-3 DATA POINT 1.1062
.0643
.1135
.0618
.9818
1.00
0.9
0.8
0.7
0.6
0.5
0.4
0.3
0.2
0.1
0
1.00
.99
.98
.97
.96
.95
.94
.93
.92
.91
A/A_c
SYMBOL
TERM
⊙
$\frac{M}{M_c}\sqrt{\frac{T_c}{T}}$
□
$\left(\frac{M}{M_c}\right)^2$

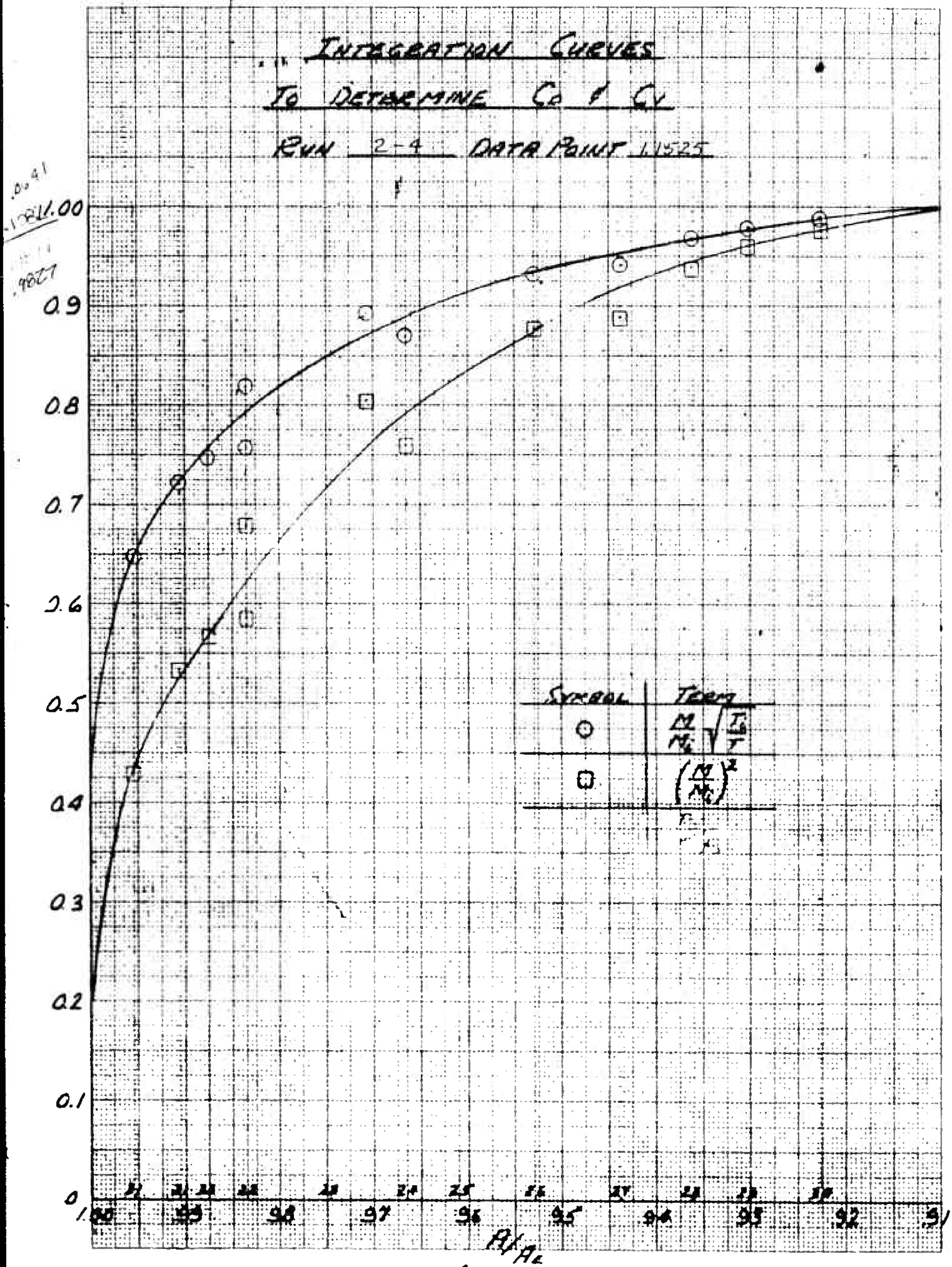
INTEGRATION CURVES
TO DETERMINE C_D & C_V
RUN 2-4 DATA POINT
1.00
0.9
0.8
0.7
0.6
0.5
0.4
0.3
0.2
0.1
0
1.00
.99
.98
.97
.96
.95
.94
.93
.92
.91
A/A_c
SYMBOL
TERM
$\frac{M}{M_i}\sqrt{\frac{T_i}{T}}$
$\left(\frac{M}{M_i}\right)^2$
.9827

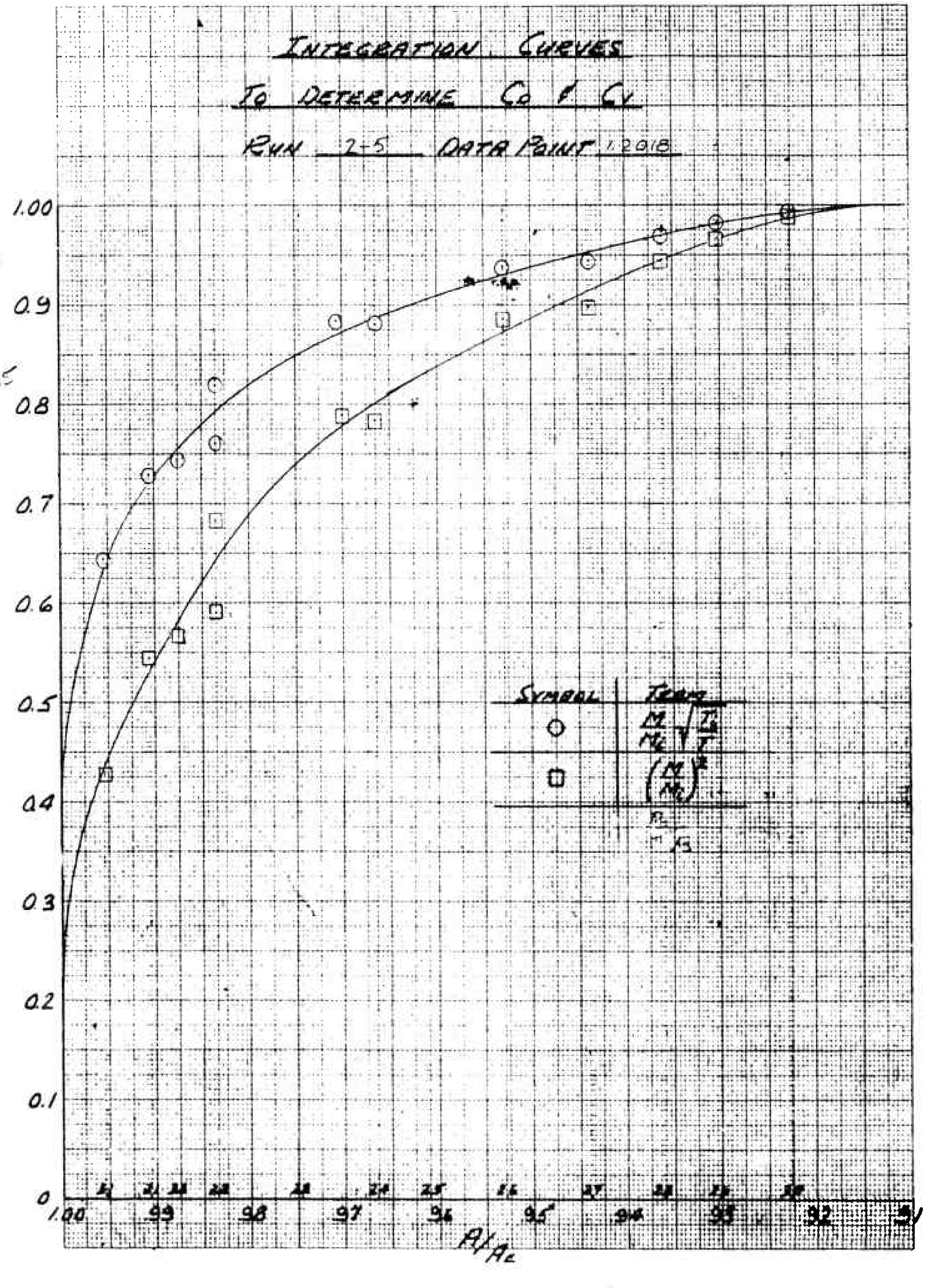

INTEGRATION CURVES
TO DETERMINE C_D & C_V
RUN 2-5 DATA POINT 12018
1.00
0.9
0.8
0.7
0.6
0.5
0.4
0.3
0.2
0.1
0
1.00
.99
.98
.97
.96
.95
.94
.93
.92
.91
A_x/A_e
SYMBOL
TERM
○ $\frac{M}{M_e}\sqrt{\frac{T_e}{T}}$
□ $\left(\frac{M}{M_e}\right)^2$

TABLE 1 TABULATED TEST RESULTS

Data Point	Press. Ratio	Po (psia)	Ps (psia)	Pa (psia)	Ps/Pa	$\int \frac{M}{M_i} \sqrt{\frac{T_i}{T}} \frac{dA}{A_E}$	$\int \left(\frac{M}{M_i}\right.$
1	1.209	17.23	14.29	14.25	1.0031	.9902	.
2	2.408	35.20	18.21	14.25	1.2779	.9923	.
3	1.418	20.14	14.28	14.21	1.0052	.9905	.
4	1.643	23.34	14.32	14.21	1.0079	.9905	.
5	1.857	26.37	14.45	14.21	1.0176	.9915	.
6	2.059	29.25	15.41	14.21	1.0848	.9921	.
8	2.276	32.23	16.79	14.42	1.1860	.9924	.
9	2.487	35.21	18.35	14.42	1.2959	.9925	.
10	2.710	38.37	20.02	14.42	1.4141	.9925	.
11	2.904	41.05	21.27	14.14	1.5052	.9923	.
12	3.120	44.09	22.83	14.13	1.6193	.9925	.
13	3.355	47.20	24.57	14.05	1.7491	.9925	.
14	3.568	50.10	26.11	14.04	1.8602	.9924	.
15	3.773	52.96	27.60	14.04	1.9662	.9926	.
16a	3.985	55.93	29.27	14.03	2.0854	.9930	.
16b	3.929	55.13	28.79	14.03	2.0513	.9924	.
17	1.219	17.12	14.07	14.04	1.0021	.9903	.
18	1.431	20.09	14.10	14.04	1.0045	.9911	.
19	1.647	23.13	14.13	14.04	1.0066	.9912	.
20	1.613	23.14	14.13	14.04	1.0063	.9903	.
21	1.859	26.10	14.28	14.04	1.0171	.9917	.
22	2.066	29.00	15.25	14.04	1.0861	.9922	.
23	2.073	29.11	15.27	14.04	1.0875	.9923	.
24	1.213	17.10	14.14	14.09	1.0035	.9908	
25	1.647	23.21	14.48	14.09	1.0278	.9918	
26	2.498	35.20	18.85	14.09	1.3373	.9928	
27	2.488	35.07	18.81	14.09	1.3348	.9925	
28	3.123	44.13	22.94	14.11	1.6260	.9927	
29	3.136	44.24	23.02	14.11	1.6319	.9925	
2-1	1.032	14.655	14.225	14.227	1.00007	.9893	
2-2	1.053	14.980	14.229	14.227	1.00010	.9900	
2-3	1.106	15.733	14.229	14.227	1.00012	.9893	
2-4	1.152	16.397	14.231	14.227	1.00027	.9897	
2-5	1.202	17.099	14.232	14.227	1.00033	.9900	

EST RESULTS

$\frac{dA}{AE}$	$\int\left(\frac{M}{Mi}\right)^2 \frac{dA}{AE}$	C_D	C_V	Cs	Thrt. Re $\times 10^{-6}$
02	.9829	.9902	.9927	1.1541	2.54
23	.9874	.9923	.9952	1.2689	7.47
05	.9840	.9905	.9953	1.2248	3.62
05	.9851	.9905	.9948	1.2592	4.66
15	.9865	.9915	.9952	1.2683	5.60
21	.9869	.9921	.9953	1.2682	6.19
24	.9879	.9924	.9968	1.2704	6.83
25	.9880	.9925	.9953	1.2680	7.47
25	.9876	.9925	.9941	1.2683	8.15
23	.9878	.9923	.9918	1.2683	8.70
25	.9880	.9925	.9888	1.2704	9.44
25	.9883	.9925	.9880	1.2686	10.0
24	.9880	.9924	.9875	1.2678	10.6
26	.9880	.9926	.9838	1.2681	11.2
30	.9885	.9930	.9819	1.2683	12.0
24	.9878	.9924	.9829	1.2683	11.9
03	.9836	.9903	.9929	1.1593	2.52
11	.9853	.9911	.9938	1.2283	3.62
12	.9855	.9912	.9939	1.2592	4.60
03	.9840	.9903	.9936	1.2587	4.60
17	.9870	.9917	.9954	1.2684	5.54
22	.9876	.9922	.9937	1.2683	6.15
23	.9876	.9923	.9957	1.2711	6.17
08	.9843	.9908	.9939	1.1554	2.53
13	.9864	.9918	.9950	1.2557	4.62
28	.9879	.9928	.9953	1.2681	7.49
25	.9878	.9925	.9955	1.2684	7.43
27	.9882	.9927	.9895	1.2681	4.51
23	.9882	.9925	.9903	1.2679	9.72
93	.9815	.9893	.9921	1.0402	0.94
00	.9818	.9900	.9917	1.0571	1.25
93	.9818	.9898	.9919	1.0968	1.73
97	.9827	.9897	.9929	1.1261	2.11
00	.9835	.9900	.9934	1.1523	2.42

2